KINEMATIC DESIGN OF SCISSOR LINKAGES

A Thesis Submitted to the
Graduate School of Engineering and Sciences of
İzmir Institute of Technology
in Partial Fulfillment of the Requirements for the Degree of

MASTER OF SCIENCE

in Mechanical Engineering

by
Cevahir Karagöz

July 2018
İZMİR

We approve the thesis of **Cevahir KARAGÖZ**

Examining Committee Members:

_____
Assoc. Prof. Dr. Gökhan KİPER
Department of Mechanical Engineering, İzmir Institute of Technology

_____
Assoc. Prof. Dr. Koray KORKMAZ
Department of Architecture, İzmir Institute of Technology

_____
Assist. Prof. Dr. Erkin GEZGİN
Department of Mechatronics Engineering, İzmir Katip Çelebi University

06 July 2018

_____
Assoc. Prof. Dr. Gökhan KİPER
Supervisor, Department of Mechanical Engineering,
İzmir Institute of Technology

_____
Prof. Dr. Metin TANOĞLU
Head of the Department of
Mechanical Engineering

_____
Prof. Dr. Aysun SOFUOĞLU
Dean of the Graduate School of
Engineering and Sciences

ACKNOWLEDGMENTS

First of all, I would like to express my deepest appreciation to my supervisor Assoc. Prof. Dr. Gökhan Kiper for his encouragement and recommendations throughout this study. I am also thankful for his endless moral support, patience and understanding that motivated me to work in the RAML Mechatronic Laboratory in peace and non-technical topics as well.

I would like to thank the members of my thesis examining committee; Assoc. Prof. Dr. Koray KORKMAZ and Assist. Prof. Dr. Erkin GEZGİN for their invaluable suggestions to complete this thesis.

I would also like to thank the members of OptArch Project; Dr. Koray Korkmaz, Dr. Gökhan Kiper, Dr. Yenal Akgün, Dr. Feray Maden, Dr. Engin Aktaş, Müjde Yar, Şebnem Gür, Kutay Yücetürk, Duhan Ölmez and Erinç Yıldırım.

I am grateful to all members of RAML Mechatronics Laboratory, Industrial Robotics Laboratory and Modelling and Simulation Laboratory for their eternal motivation.

And above all, my deepest appreciation goes to my valuable family; Ceren, Muradiye and Mustafa KARAGÖZ for their never-ending support, continuous love and encouraging me throughout all my education.

ABSTRACT

KINEMATIC DESIGN OF SCISSOR LINKAGES

The primary objective of this thesis is to propose a design method for linkages simulating the transformation of a planar curve from an initial form to a final form. First, the topologies of fundamental loops are examined using symmetry patterns. Design methodologies for the hence obtained mechanisms are formulated. The given curves are discretized initially, and the nodes are constructed. Then the side lengths of the loops are obtained in order to obtain the desired transformation between the given curves. Finally, different deployable and transformable linkage examples are presented.

ÖZET

MAKAS MEKANİZMALARININ KİNEMATİK TASARIMI

Bu tezin temel amacı başlangıç ve son formu verilen bir düzlemsel eğrinin dönüşümünde kullanılacak kollar için bir tasarım metodu sunmaktır. İlk olarak, simetri kullanılarak temel döngülerin topolojileri incelenmiştir. Böylece elde eldilen mekanizmalar için tasarım metodojileri elde edilmiştir. Verilen eğriler kesikli hale getirilmiş ve düğüm noktaları yerleştirilmiştir. Sonra, verilen eğriler için istenen dönüşümü sağlayacak olan döngülerin kenar uzunlukları elde edilmiştir. Son olarak, farklı katlanabilir ve dönüştürülebilir eklem örnekleri sunulmuştur.

TABLE OF CONTENTS

LIST OF FIGURES

LIST OF TABLES

CHAPTER 1

INTRODUCTION

Mobility and adaptability are frequently demanded for today's engineering structures. Deployable designs are required for compact transportation or storage in applications such as outer-space structures. Adaptability for different functions or changing environmental conditions is required in some architectural designs. Considering these conditions, mobile structures are finding wider area of application in different fields of study. Production methods, material types and design and analysis methods for mobile structures are still being developed today.

The "mobile structure" expression seems to contain two contradicting terms, since in general a structure is assumed to be immobile. What is meant by a mobile structure is an assembly, which acts as an immobile structure at different configurations, but which is also has mobility in order to be able to be reconfigured between different forms. Mobile structures can be classified in two main sub-categories: deployable and transformable structures. Deployable structures have at least one compact and one deployed form, whereas transformable structures may attain arbitrary forms. Although usually deployable structures have similar geometry in the compact and deployed forms, otherwise is also possible.

One of the oldest and most commonly used type mobile structures comprise scissor linkages. Scissor-like linkages (SLEs) have been used for tens of centuries in designing household goods such as deployable tables (Figure 1.1) and portable shelters. Scissor-like linkages may be a planar linkage such as the ones used for awnings (Figure 1.2) or deployable gates (Figure 1.3). On the other hand, in several examples of structures comprising scissor linkages, the linkages lie on intersecting planes as sub-assemblies. Nevertheless, in either case scissor linkages can be analyzed and designed by confining oneself to the plane.

Figure 1.1. Ancient roman tripods
(Source: © Pinterest, 2018)

Figure 1.2. Scissor awning
(Source: Central Awnings, 2016)

Figure 1.3. Pair retail window gate
(Source: Illinois Engineered Products, 2016)

The main advantages of scissor mechanisms are compactness and modularity. A system of several scissor mechanisms has the properties of a single scissor unit multiplied as many times as the number of units. For example, a translational scissor unit has same expansion properties with a single unit, the expansion ratio is the same, but the amount of expansion is as many times as the number of units. The kinematic equations of a system of scissors is much simpler compared to a system of another mechanism type. The compactness is that the scissor mechanisms have the same expansion ratio within less space.

This thesis aims to devise design methodologies for planar mobile structures comprising scissor mechanisms. Unlike many of the studies in the literature, the structural synthesis of the scissor linkages is performed by considering loops as modules. Alternative topologies of these loop assemblies are investigated mainly based on frieze groups (symmetric patterns on curves) by discretization of the desired forms of curves and the kinematic dimensions of the hence obtained scissor-like elements are

calculated by dimensional synthesis. Various deployable and transformable structure examples are worked out as case studies.

1.1. Problem Definition

This thesis study is part of the Horizon 2020 Marie Skłodowska-Curie Research and Innovation Staff Exchange 2015 project "Optimization Driven Architectural Design of Structures" (OptArch – H2020-MSCA-RISE-2015-689963) work package "Optimized Hybrid Kinetic and Adaptive Structures" leaded by İzmir Institute of Technology. The main purpose of the project is to develop an assistance optimization tool for the geometric and structural design of adaptive architectural structures. The optimization can be considered in different stages such as kinematic optimization and structural optimization. The required topologies for scissor linkage-based structures have already been classified by other researchers. This thesis is on the dimensional synthesis of these various topologies considering the desired motion of the structure.

The essential problem in this thesis is how to obtain the kinematic dimensions of the SLEs of a scissor linkage that can provide the motion for a given curve with its initial and final form using some fundamental loops. For this reason, the first step of the problem is to examine the desired motion of the structure which is idealized as a curve. The second step of the problem is to determine the proper fundamental loops for the desired curve motion. The final stage is the dimensional synthesis of the scissor linkages.

1.3. Literature Review

This section presents the state-of-the-art, contributions to engineering and architecture and the deficiencies reported in the literature. The main characteristics and the geometric properties of the existing designs are examined. The examples are selected to show the most common, important and well-known designs.

1.3.1. Deployable Structures

The structures that could be transformed from a pre-determined stowed configuration to a pre-determined expanded configuration are called deployable structures. These structures are stable and could carry external and internal loads (Hernández Merchan, 1987; Gantes, 2001) Deployable structures are mostly used in portable or temporary applications for easy storage and transportation. Additionally, they are also used to facilitate assemblies for large structures (Figure 1.4).

Figure 1.4. Rapidly Deployable engineered membrane structures
(Source: © Sprung Instant Structures, 2018)

In many areas which may have changing requirements such as weather, load or size conditions, these structures could be utilized. Deployable structures could be integrated either into a space shuttle as a deployable solar panel or a deployable space antenna to minimize its volume (Figure 1.5), an environment friendly building as a deployable roof for changing solar energy conditions or a deployable bridge in order to respond changing transportation requirements (Figure 1.6).
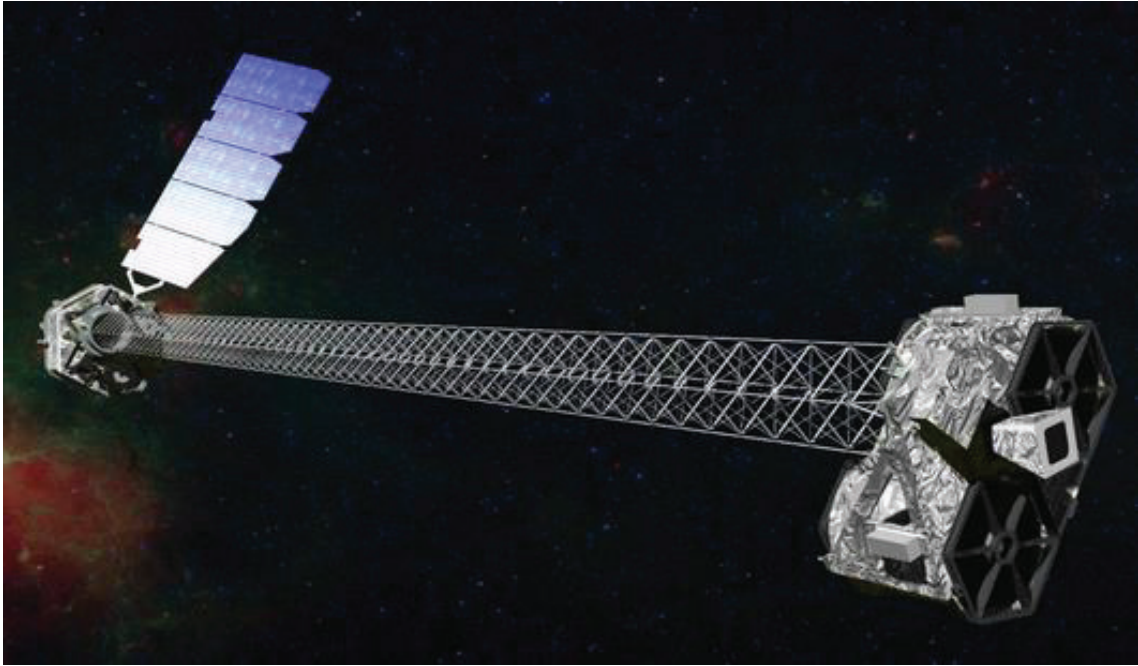
Figure 1.5. Nuclear Spectroscopic Telescope Array with Deployable Mast
(Source: © NASA/JPL-Caltech 2017)
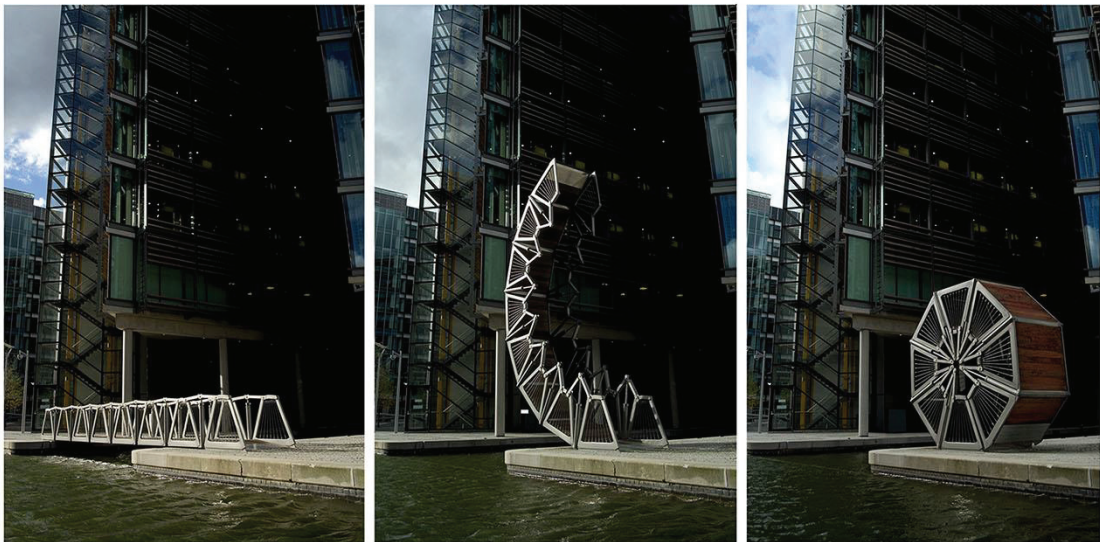
Figure 1.6. Opening steps of Rolling Bridge
(Source: Heatherwick Studio, 2018)

Well-known researchers in deployable structures area such as Pinero, Hoberman, Escrig, Valcarcel, Gantes and Pellegrino have proposed differents systems

using scissors-hinge structures. In the design and application of deployable structures in architecture, Emilio Perez Pinero is distinguished as one of the first publishers. A deployable structure comprising SLEs to construct a movable theatre is presented by Pinero (Figure 1.7). Pinero designed a scissor mechanism, but the mechanism is not stable by itself after the deployment and it needs cables to be stable (Pinero, 1961a).
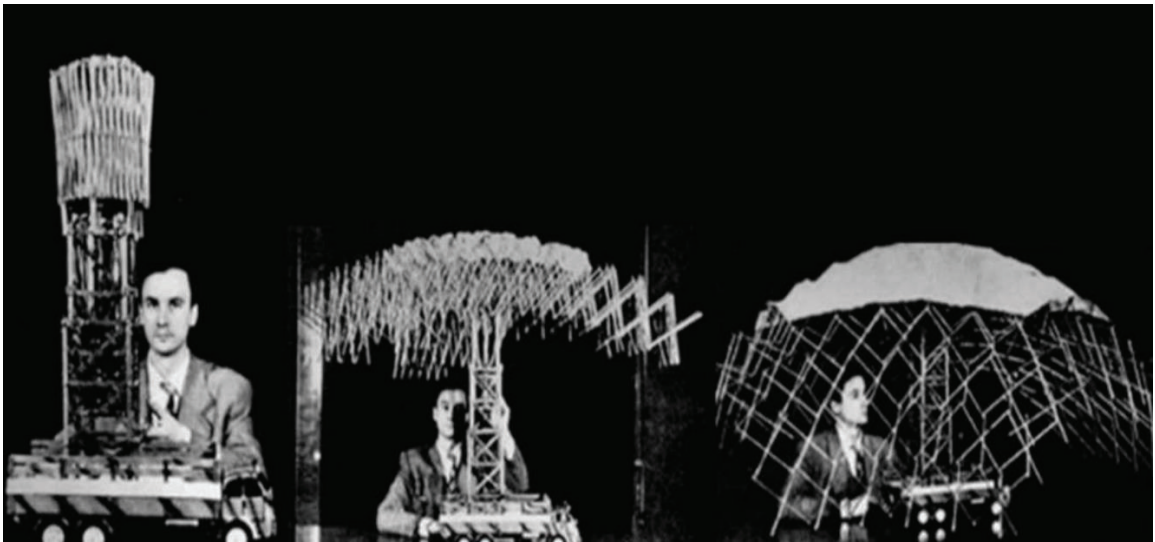
Figure 1.7. Movable Theatre
(Source: Yar, 2016)

Later works of Pinero such pavilions, temporary enclosure and retractable domes all depend on SLEs (Pinero, 1961b; Pinero, 1965). Another work is the foldable reticular dome which contains 7 modules expanding from compact bundles (Figure 1.8).
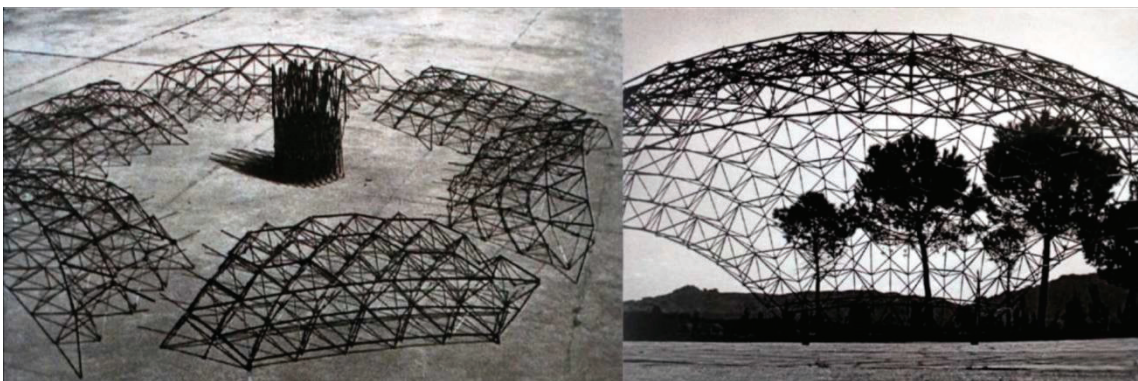
Figure 1.8. Foldable Reticular Dome
(Source: Yar, 2016)

Another pioneer in this field, Felix Escrig, worked on deployable bar structures in detail. Escrig presented not only SLE's geometric and deployability conditions but also the relation between the elements and the span of the structure (Escrig, 1985). In these studies, he focused on obtaining different geometries by using the same type of struts and different connection elements (Figure 1.9).
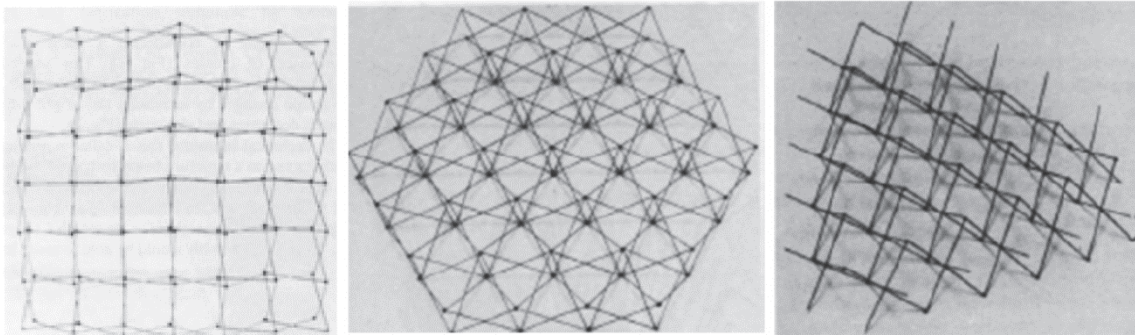
Figure 1.9. Different Geometries of Deployable Structures
(Source: Akgün, 2010)

Escrig also explained how to generate three-dimensional structures which contain planar translational SLEs in multiple directions on a grid (Figure 1.10).
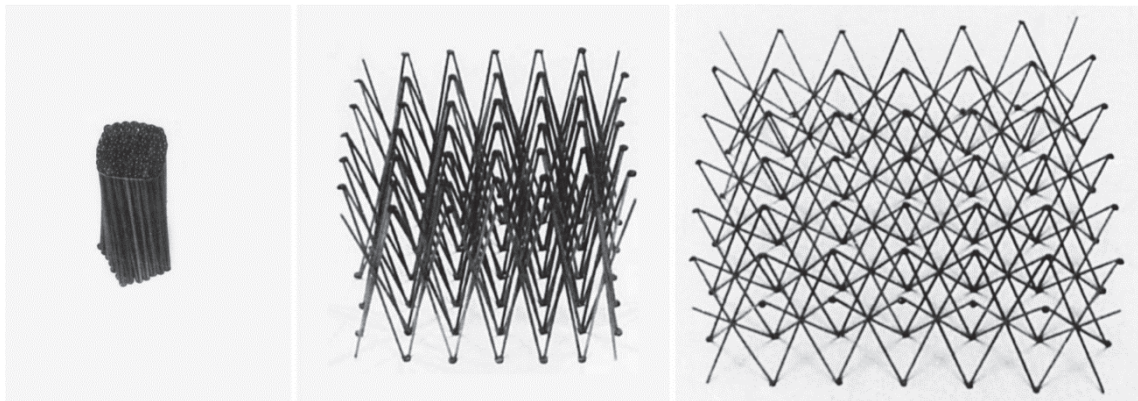
Figure 1.10. Multiway Grid Composed of Translational Scissor Unit
(Source: Gür, 2017)

Another work presented by Escrig depends on curved grids (Figure 1.11). This structure contains polar units which deploy along an arc and these units could form curved surfaces that can be stowed (Escrig, 1985).
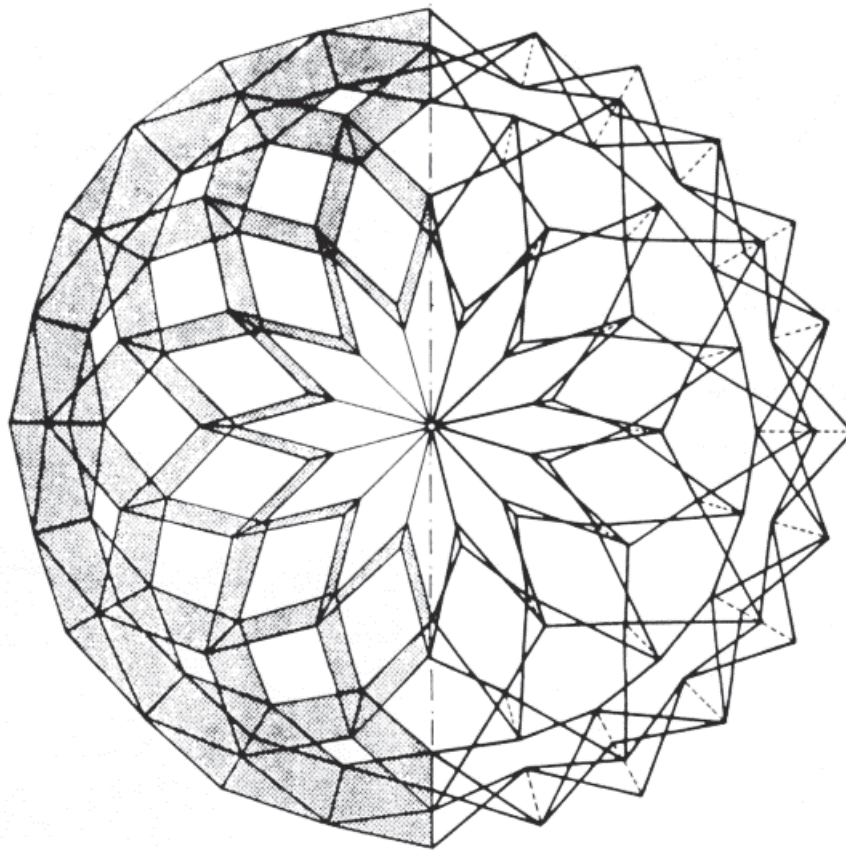
Figure 1.11. Perfect Hemispherical Dome
(Source: Escrig, 1985)

In later studies of Escrig with Valcarcel, new spherical grid structures using two-way and three-way scissors are developed (Escrig and Valcarcel, 1986a; Escrig and Valcarcel, 1986b; Escrig and Valcarcel, 1987). The other works developed by Escrig and Valcarcel are spherical and geodesic structures, quadrilateral expandable umbrella, deployable polyhedral and compact folded cylinder (Escrig and Valcarcel, 1993).

Another valuable work of Escrig and Valcarcel is the rigid plate roofing element. Deployable structures have been covered with a thin fabric roof which does not contribute to structural strength in general. Escrig designed deployable structures which contained rigid plates using as part of the mechanism (Figure 1.12). In this design, the plates overlap with each other (Robbin, 1996).
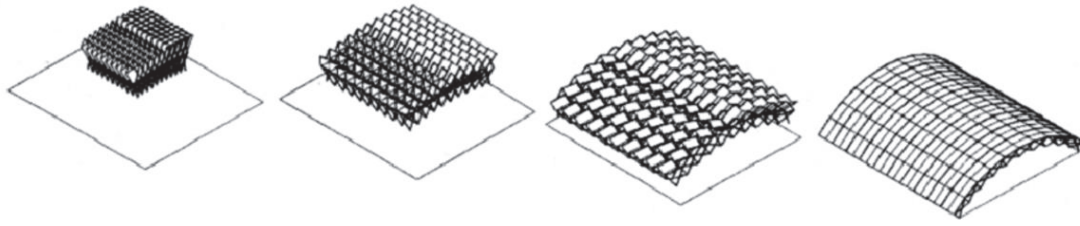
Figure 1.12. Deployable Plate Structures
(Source: Akgün, 2010)

Deployable roof structure for a swimming pool in San Pablo Sports Centre in Seville, Spain by Escrig (1996) is one of real-life application of scissors units applied. This roof structure is based on two identical rhomboid grid structures covered with fabric (Figure 1.13, Figure 1.14).
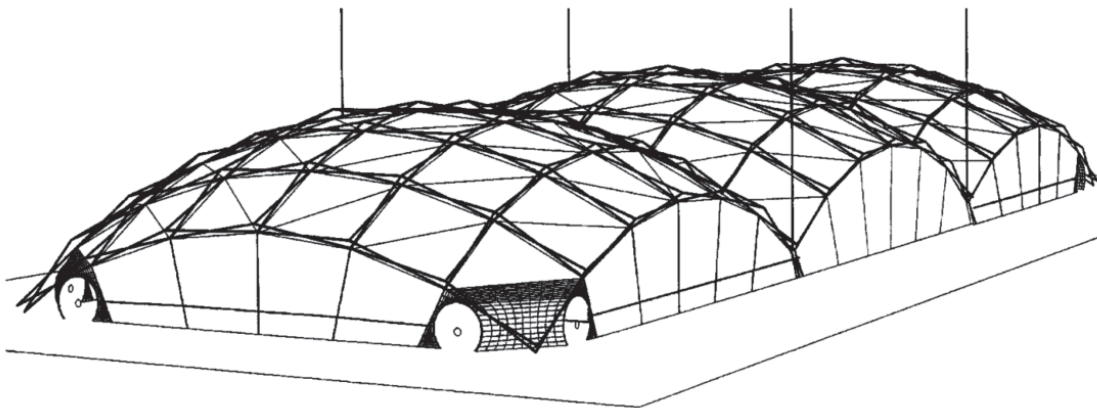
Figure 1.13. Swimming pool in Seville
(Source: Kassabian et al., 1999)

Langbecker (1999) developed the foldability conditions of SLEs and work on the deployability and kinematics of translational, cylindrical and spherical configurations of scissor structures. Langbecker also developed barrel vaults (Langbecker and Albermani, 2001). Many models of singly-curved foldable barrel vaults and doubly-curved synclastic and anticlastic structures (Figure 1.15) (Langbecker and Albermani,2000).

Figure 1.14. Deployable swimming pool
(Source: © Grupo Estran, 2018)
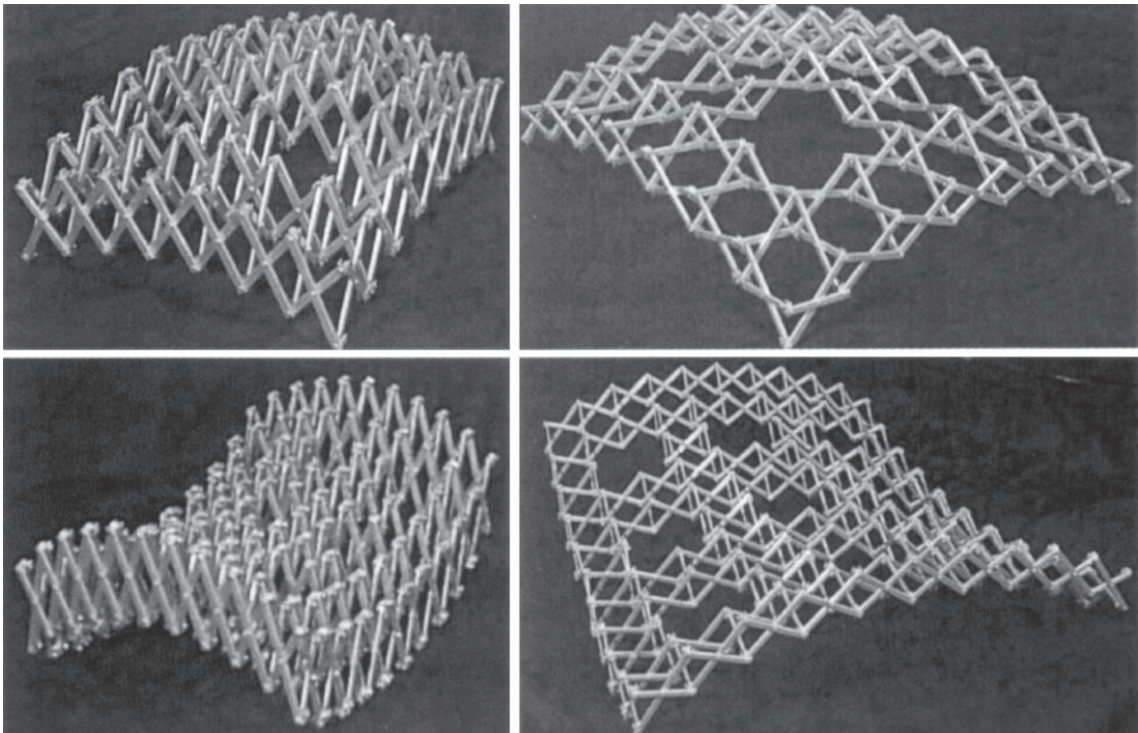
Figure 1.15. Synclastic and Anticlastic structures
(Source: Akgün, 2010)

In all examples presented so far, the basic unit of the assembly can be considered as a pair of ternary links with revolute joints only for which the joint axes are coplanar, or to say, hinge points are collinear as in the so-called translational or polar units shown in Figure 1.16 as the left and mid figures. Besides these two well-known types of scissor pairs in the literature, Chuck Hoberman discovered a new type of SLE: the angulated element, where the three hinge points on a link are not collinear,

11

but rather form a triangle (right figure in Figure 1.16). With his work on angulated scissors, Hoberman developed many structures. Some well-known structures are the Hoberman sphere (Hoberman, 1990) (Figure 1.17), Iris Dome (Hoberman, 1991) (Figure 1.18) and Hoberman Arch at 2002 Winter Olympics (Figure 1.19).
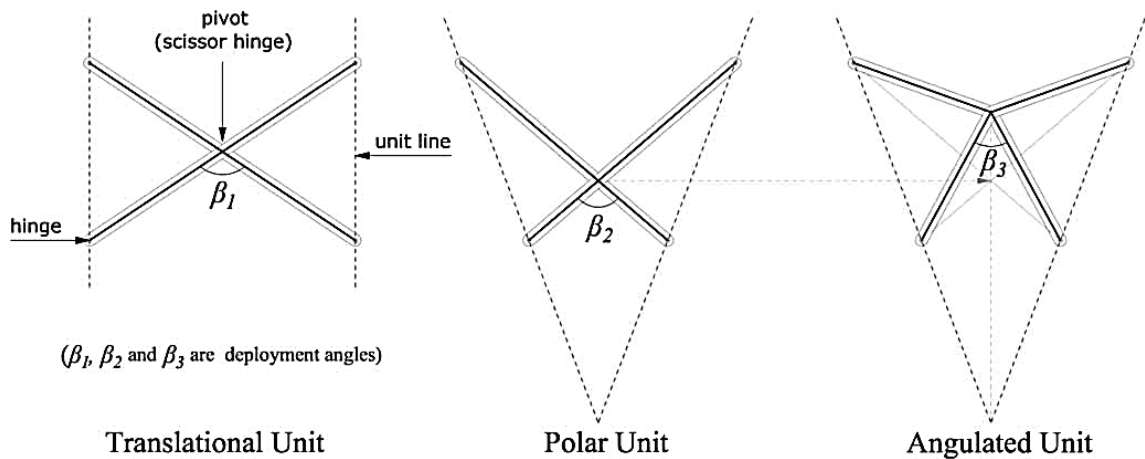
Figure 1.16. Translational, polar and angulated units
(Source: Maden, Korkmaz and Akgün, 2011)

Figure 1.17. Hoberman sphere
(Source: Wikipedia, 2018)

Figure 1.18. Open and Closed Form of Iris Dome
(Source: Google Images, 2018)
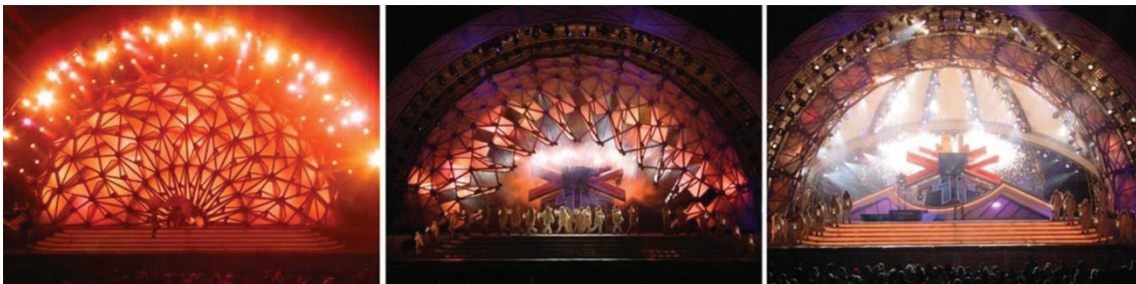
Figure 1.19. Hoberman Arch in 2002 Winter Olympics
(Source: Google Images, 2018)

Sergio Pellegrino and Zhong You examined angulated scissors in detail. They investigated not only pairs of identical links, but also different link pairs and they discovered equilateral and similar generalized angulated elements (GAEs) (Figure 1.20) (You and Pellegrino, 1997). Reducing the number of components of the structure and the complexity of joints, multi-angulated element (multi-AE) was discovered by You and Pellegrino (Figure 1.21).

Van Mele (2010) covered a tennis arena by using scissors arches composed of angulated elements. Two angulated scissor arches carried by pin connected arches make a barrel vault (Figure 1.22).
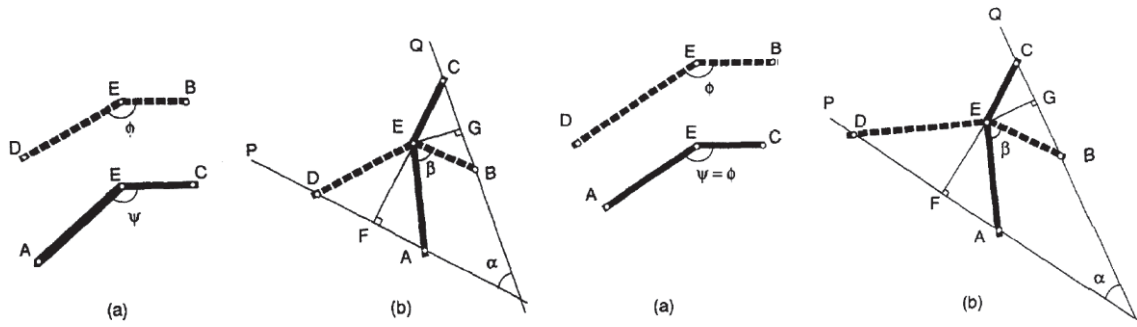
Figure 1.20. Equilateral GAE (AE = DE, BE = CE, $\phi \neq \psi$) and similar GAE
(Source: You and Pellegrino, 1997)
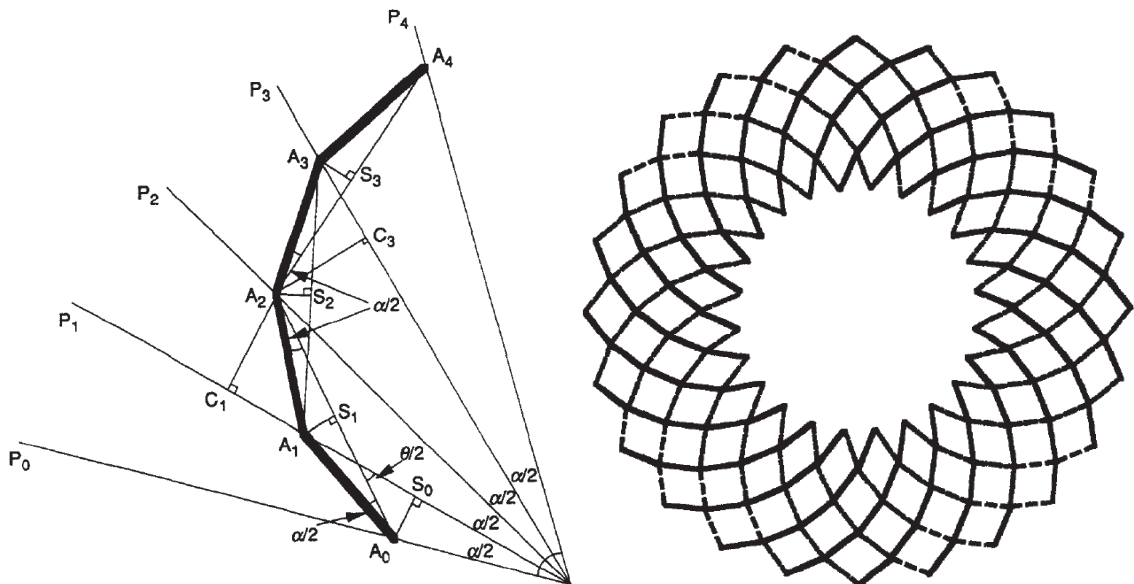
Figure 1.21. A multi-AE and a ring-like structure with multi-AEs
(Source: You and Pellegrino, 1997)

The study of Rippmann is a little different from the previous studies mentioned above. He presented a transformable structure design with high deployable ratio. Rippmann obtained the curved structures using non-identical scissor units (ROK, 2018). He used a scissor unit design with adjustable intermediate hinge point locations (Figure 1.23) (Figure 1.24).
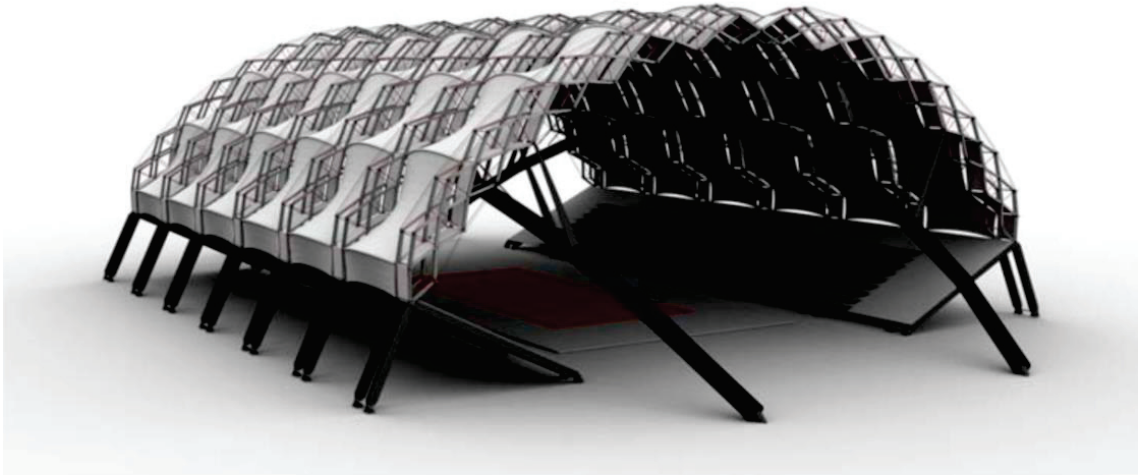
Figure 1.22. A scissor-hinged retractable membrane roof
(Source: Van Mele et al., 2010)
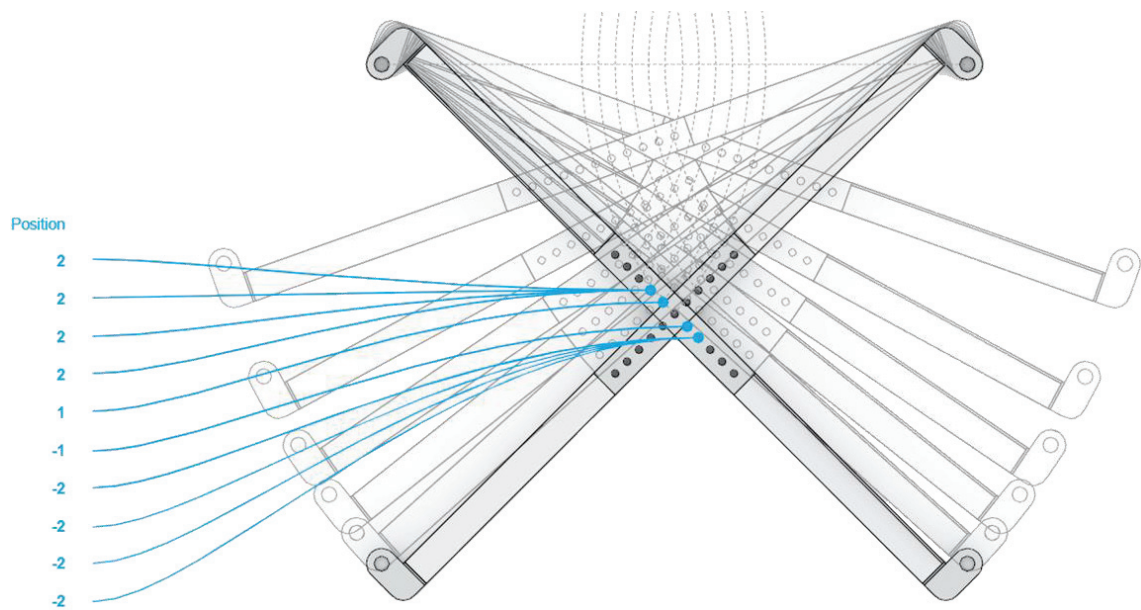
Figure 1.23. Scissor unit with adjustable hinge location
(Source: ROK, 2018)
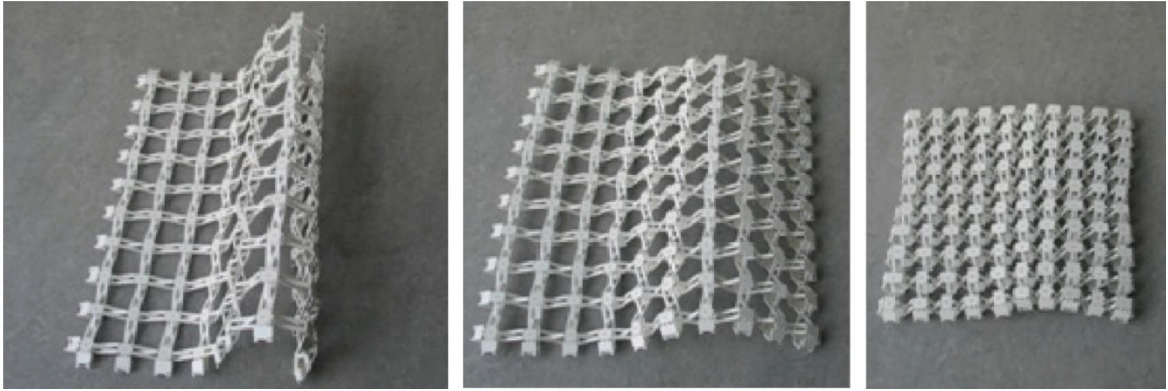
Figure 1.24. Rippmann's scissor structure
(Source: Akgün, 2010)

Liao and Li (2005) (Figure 1.25) and Kiper and Söylemez (2010) (Figure 1.26) have devised methodologies for scaling planar graphs or loops. Both approach results in linkages with rhombus loops
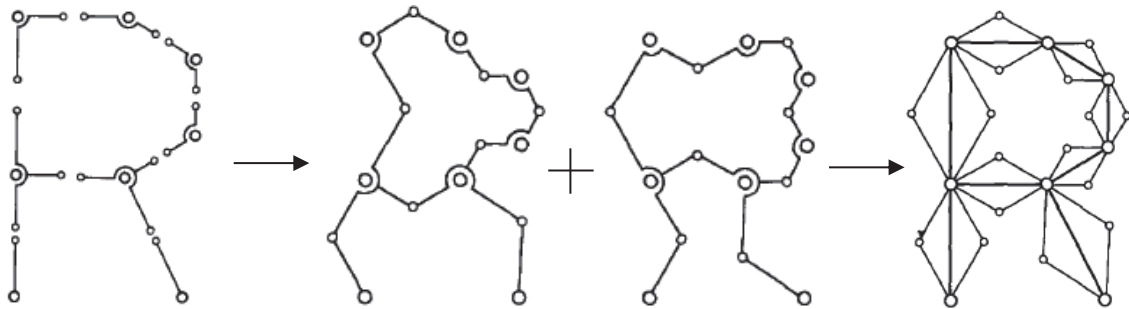
Figure 1.25. Liao and Li's scaling linkages
(Source: Liao et al., 2005)

A recent study on design of scissor linkages by Zhang et al. (2016) presents a design methodology for transformation between arbitrary curve shapes (Figure 1.27). Their design is based on scissor units with preserved or varied subtended angles.

Instead of using scissor units for designing scissor linkages, an alternative approach is using loops as modules and assembling the loops. Such a method can be called as loop assembly method. Although it is not explicitly specified in the patent, the loop assembly method is first implemented by Hoberman (1990). Later on, Hoberman (2013) explains his methodology in detail in an invite4d lecture at MIT (Figure 1.28). What he simply does is to install rhombi on the sides of a polyline.
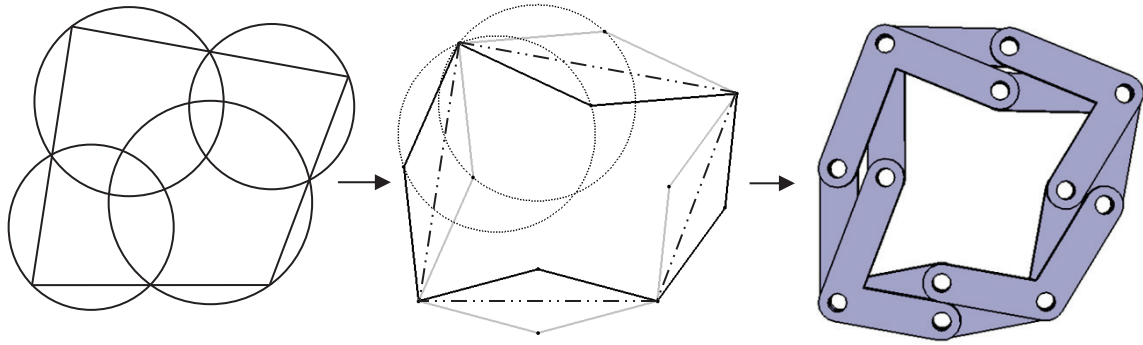
Figure 1.26. Kiper and Söylemez's polygon scaling linkages
(Source: Kiper et al., 2010)
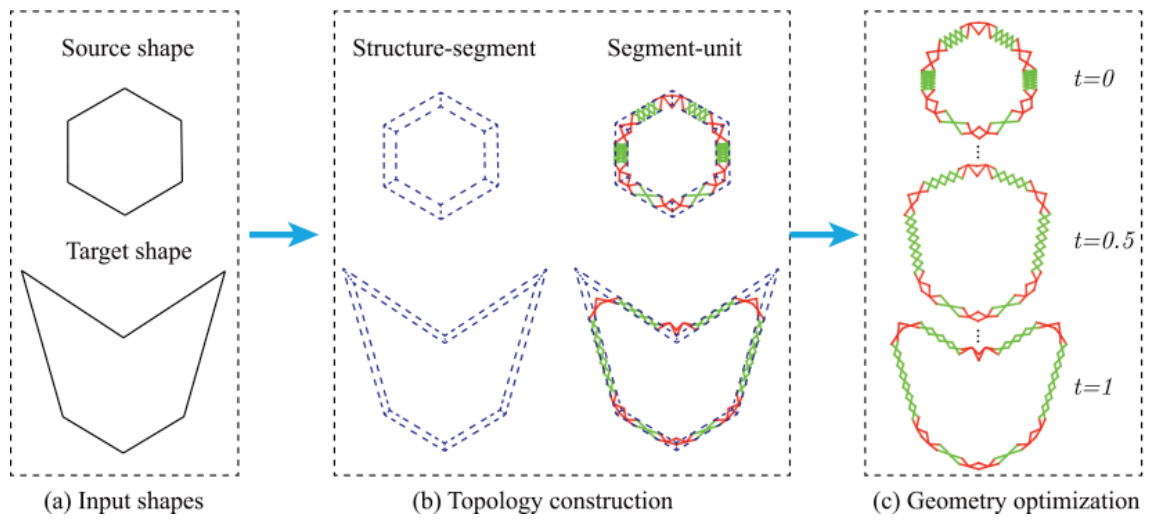
Figure 1.27. Zhang et al.'s design methodology
(Source: Zhang et al., 2016)
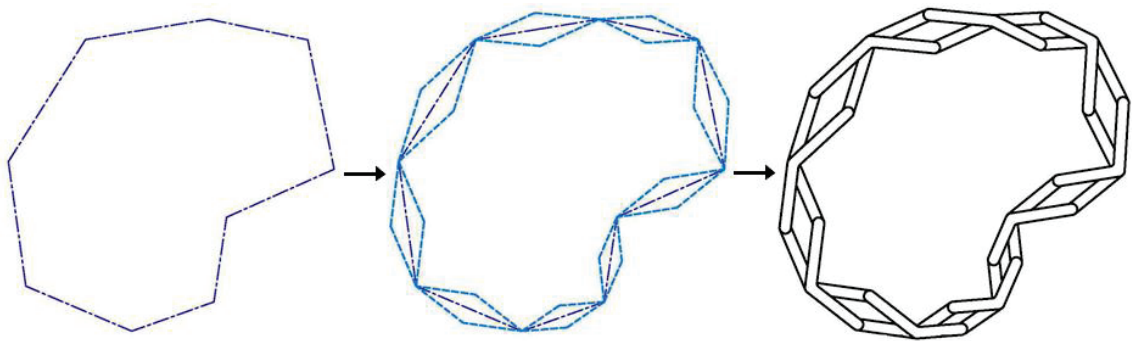
Figure 1.28. Hoberman's design methodology
(Source: Hoberman, 2013)

The loop assembly method is later further generalized for other loop types by Bai et al. (2014) using kite, parallelogram and general tetragon loops (Figure 1.29).

Rhombus

Kite

Parallelogram

General Tetragon
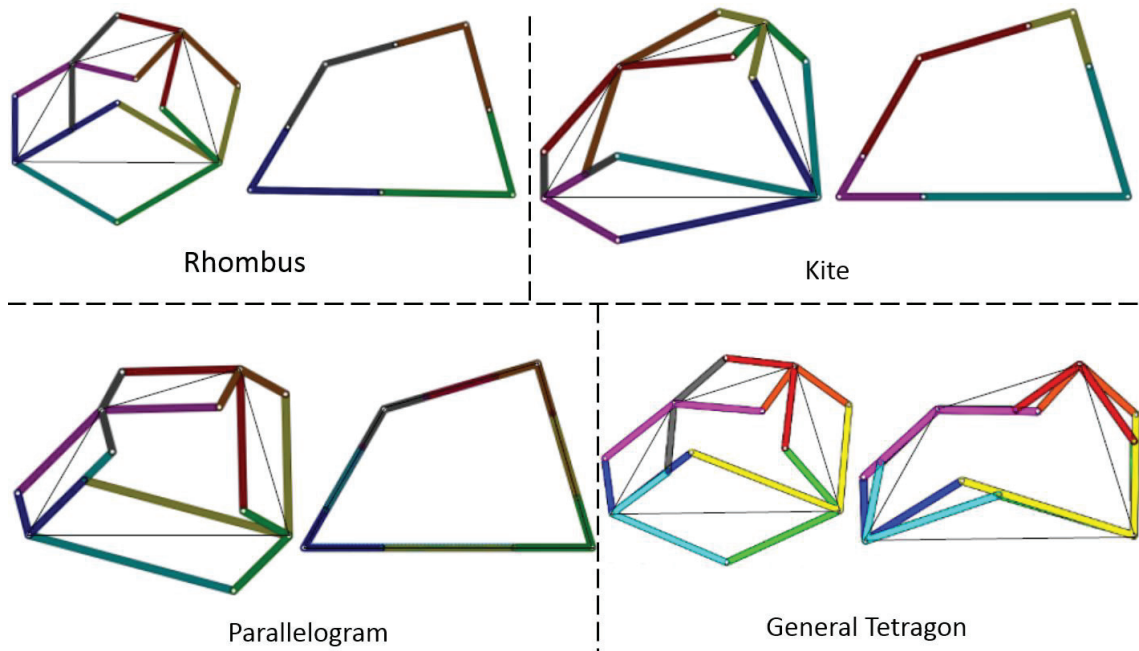
Figure 1.29. Bai et al.'s scaling linkages
(Source: Bail et al., 2014)

Recently, the loop assembly method is used with dart (concave kite) and anti-parallelogram loops by Yar et al. (2017) and Gür et al. (2017, 2018), respectively (Figures 1.30-1.31). This thesis is a result of the research conducted by this research group as well.

1.4. Methodology

In this thesis, the dimensional design method is devised for approximating the motion of a curve transforming between an initial and final form using scissor linkages comprising some fundamental loops. First, the topology of the fundamental loops are examined using symmetry groups on curves. The joints of the obtained mechanisms are located in the nodes obtained by discretizing the curves. This placement is done by inserting suitable fundamental loops on the curve. Finally, the dimensional design of the SLEs is performed.
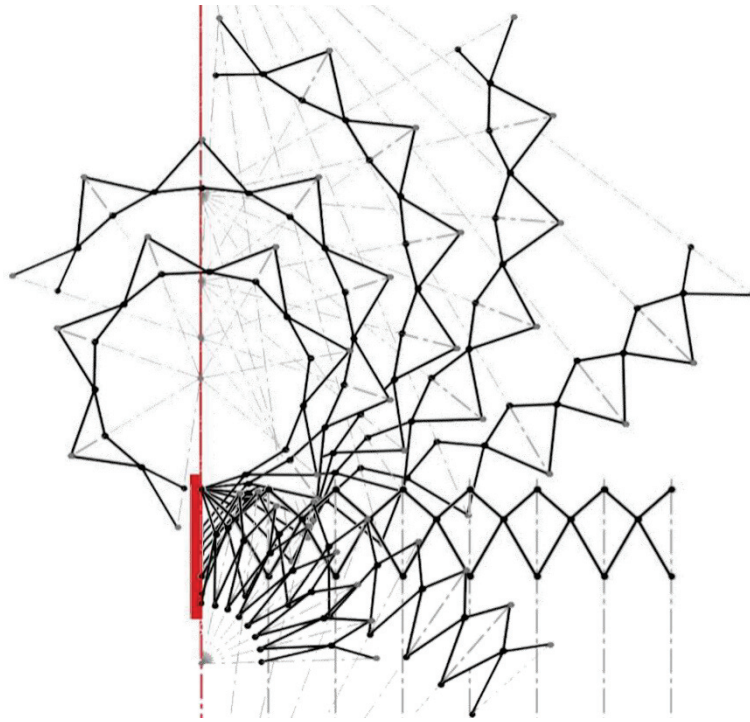
Figure 1.30. Concave kite loop assembly
(Source: Yar et al., 2017)
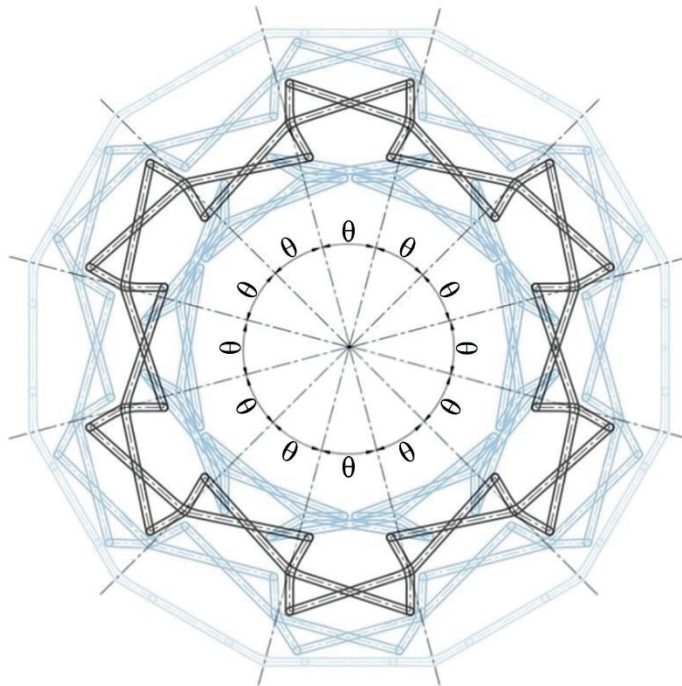
Figure 1.31. Antiparallelogram loop assembly
(Source: Gür et. al., 2017)

1.5. Summary of the Chapters

In Chapter 2, first an introduction to the fundamental loops in the literature is presented (Section 2.1) and a classification of alternative mechanism topologies is presented using the symmetry groups on a curve (Section 2.2). The introduction part of Chapter 3 contains the discretization of the given curves. A scaling deployable structure example is given in Section 3.1. An angular deployable structure example is given in Section 3.2 and a transformable structure example is given in Section 3.3. Conclusions are presented in Chapter 4.

CHAPTER 2

STRUCTURAL DESIGN

This Chapter first presents the fundamental loops and their assemblies (patterns). These assemblies are produced by using symmetry groups on curves. Then link geometries are decided based on the patterns. The hence-obtained linkages are also tabulated.

2.1. Loops

When the assemblies of scissor-like elements in the literature are examined, the following loops are dominant: kite, parallelogram and rhombus. Kite is a convex quadrilateral with two pairs of equal lengths where the long (b) and short (a) sides are adjacent (Figure 2.1).
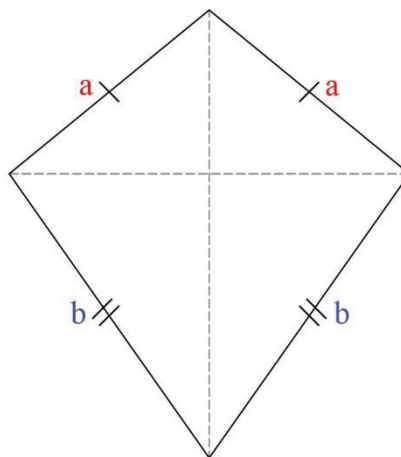
Figure 2.1. Kite Loop

Parallelogram is also a convex quadrilateral with two pairs of equal lengths where opposite sides are equal (Figure 2.2).
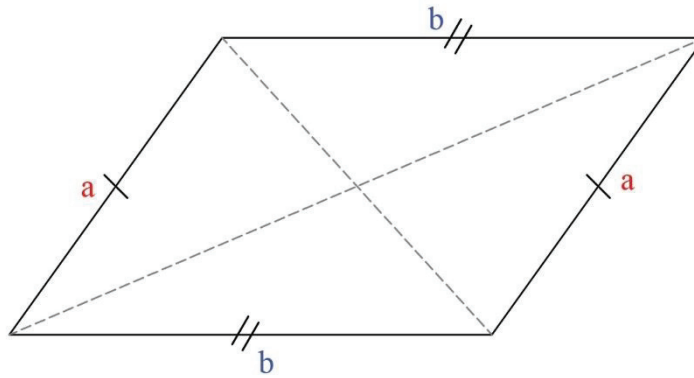
Figure 2.2. Parallelogram Loop

Rhombus is the special case of both of these two loops with four equal sides. Rhombus can be regarded as a kite or a parallelogram with equal short and long sides (Figure 2.3).
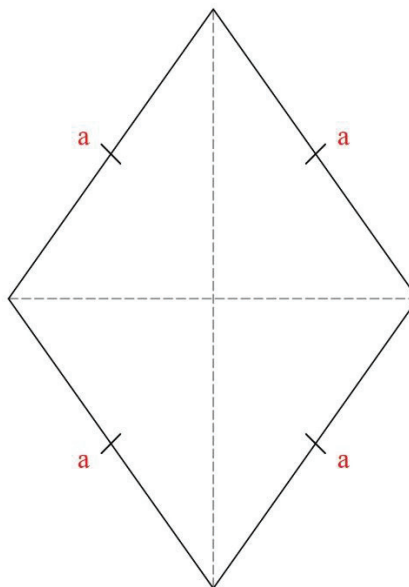
Figure 2.3. Rhombus Loop

Although a random quadrilateral has four different side lengths, a kite or a parallelogram has only two different side lengths. This condition of the side lengths provides a special geometric constraint in the design of deployable structures. Actually, this is the prominent over-constraint condition for these linkages. At this point, two other loops with two identical long sides and two identical short sides could be detected.

Although the first three examples are convex, the two other loops are concave. These are the dart loop which could be considered as a concave kite (Figure 2.4) and anti-parallelogram which could be also considered as a concave parallelogram (Figure 2.5). Unlike kite and parallelogram loops, dart and anti-parallelogram loops do not have the special case as rhombus loops.
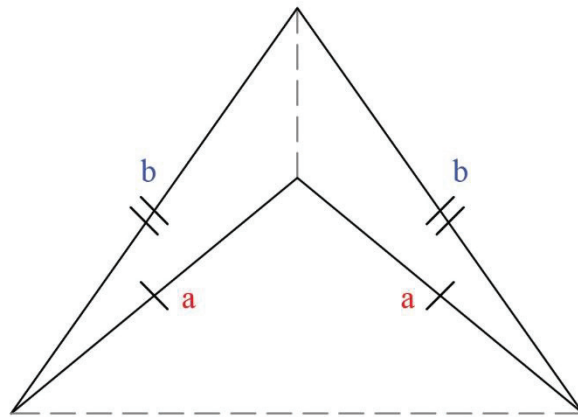
Figure 2.4. Dart Loop
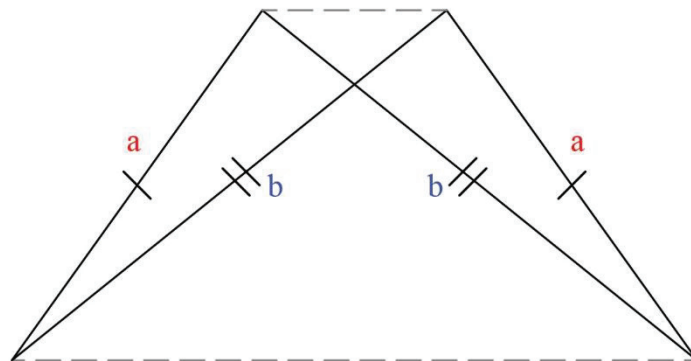
Figure 2.5. Antiparallelogram Loop

If quadrilaterals are simply considered as a 4-bar loop, the kite loop and dart loop could be perceived as different assembly modes of the same 4-bar loop. In the singular configuration where two short links are inline, the assembly mode of a kite loop could change to a dart loop (Figure 2.6).

23
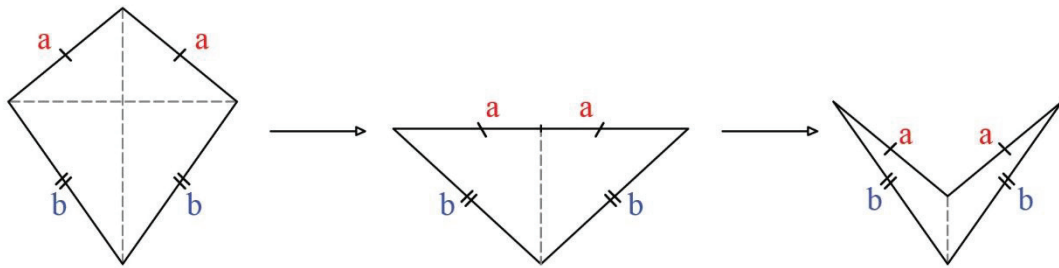
Figure 2.6. Assembly mode change of a kite loop (left) into a dart loop (right) through the singular configuration (middle)

Similarly, a parallelogram also has two assembly modes where the assembly mode change occurs when all links are collinear at the singular configuration (Figure 2.7).
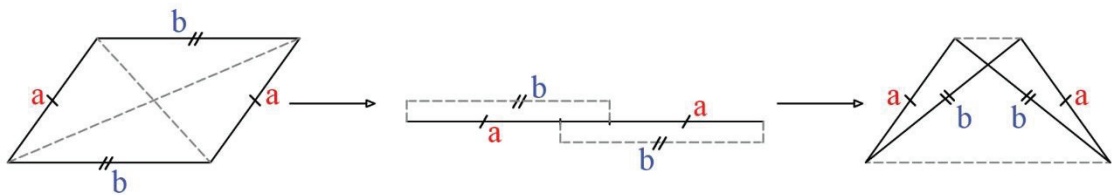
Figure 2.7. Assembly mode change of a parallelogram (left) into an anti-parallelogram (right) through the singular configuration (middle)

In a multi-loop assembly, loops could constrain each other. Hence, the assembly mode change may not occur even though some loops are in singular configurations. Also, assembly changes may not be possible due to link collisions in real applications.

2.2. Loops Assemblies and Linkage Topologies

A frieze pattern is a design on two dimensional surfaces that are repetitive in one direction. These patterns are frequently encountered in architecture and decorative arts. A frieze group is basically the symmetry set of these frieze patterns. Mathematical studies on frieze pattern have shown that these patterns can be classified into 7 types.

24

These patterns are based on 4 main symmetry operations. Translation, rotation, reflection and glide reflection (Figure 2.8) (Gür, 2017).
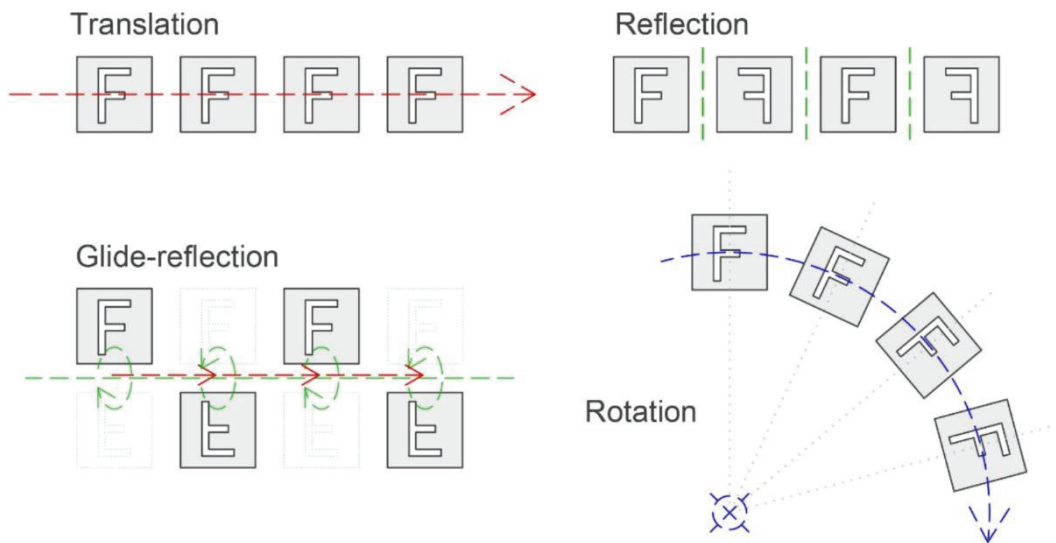
Figure 2.8. Main symmetry operations
(Source: Gür, 2017)

These 7 types are Hop (Figure 2.9), Step (Figure 2.10), Sidle (Figure 2.11), Dizzy Sidle (Figure 2.12), Dizzy Jump (Figure 2.13), Jump (Figure 2.14) and Spinning Jump (Figure 2.15) (Conway et al., 2008).
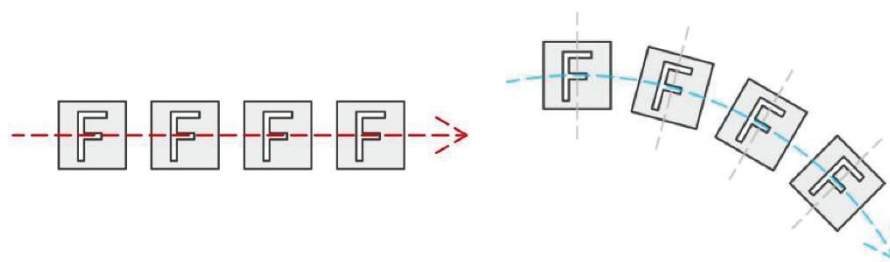
Figure 2.9. Hop (F1)
(Source: Gür, 2017)
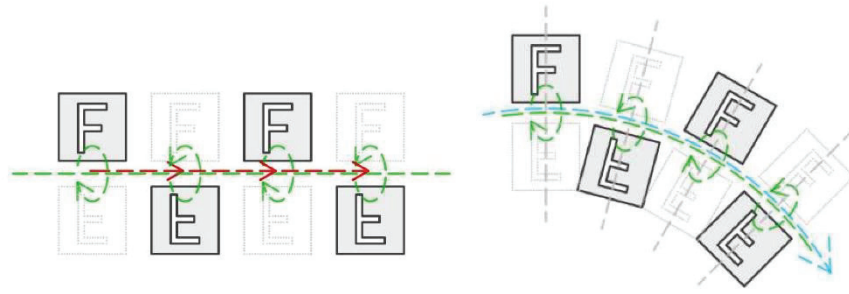
Figure 2.10. Step (F2)
(Source: Gür, 2017)
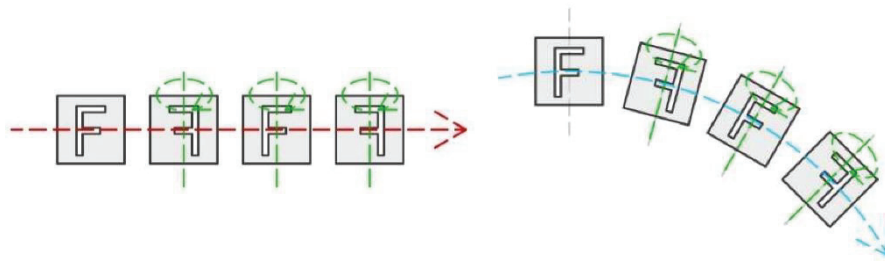
Figure 2.11. Sidle (F3)
(Source: Gür, 2017)
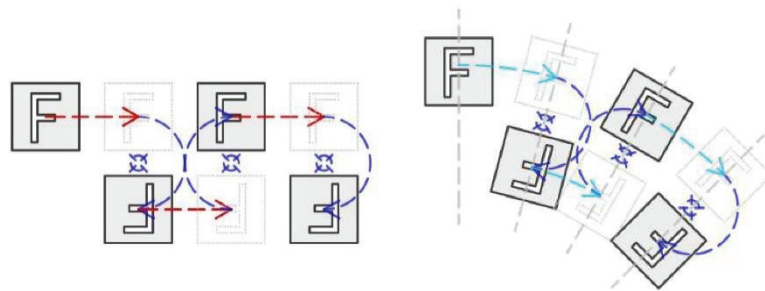
Figure 2.12. Dizzy Sidle (F4)
(Source: Gür, 2017)
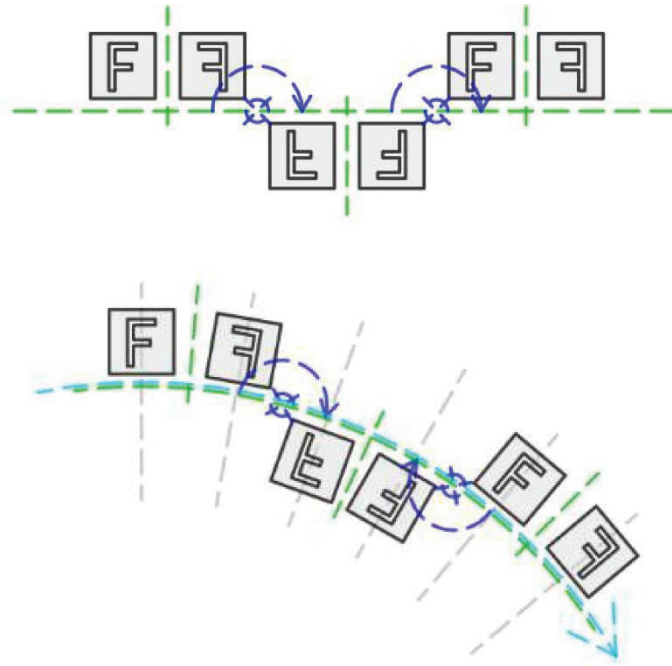
Figure 2.13. Dizzy Jump (F5)
(Source: Gür, 2017)
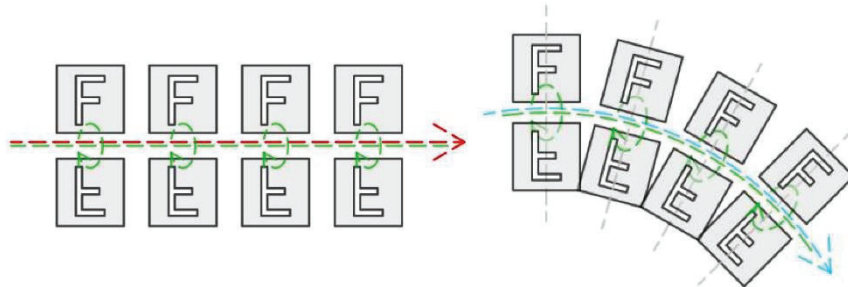
Figure 2.14. Jump (F6)
(Source: Gür, 2017)
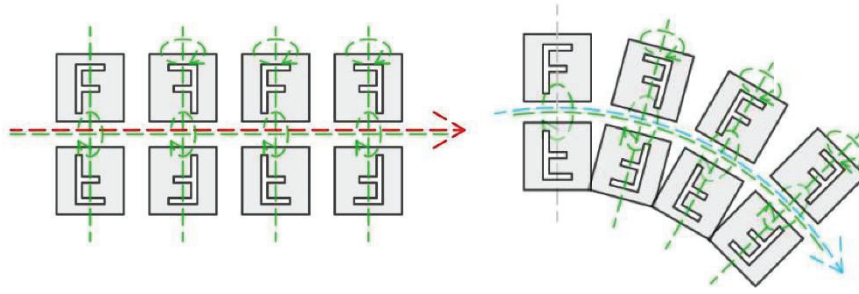
Figure 2.15. Dizzy Jump (F7)
(Source: Gür, 2017)

In a scissor linkage, there are no two rows on top of each other. Therefore Jump (F6) and Spinning Jump (F7) patterns are unrelated to this study.

Using these frieze patterns, Gür and Yar (2018) have created several scissor linkage assemblies for dart (Figure 2.16), kite (Figure 2.17), parallelogram, rhombus and anti-parallelogram loops. Motion studies have been conducted by examining the movements of these assemblies. Although the patterns are obtained for identical loops, non-identical loops may be multiplied on a curve as well.

In this study, the observed movements are evaluated to detect general and specific cases. The detected motions can be classified under 3 fundamental types: Scaling Type Deployment (up figure in Figure 2.18), Angular Deployment (middle figure in Figure 2.18) and Transformability (down figure in Figure 2.18) (Kiper, 2018).

Unclassified movements are also investigated and some of these movements are structurally similar. These similarities are attributed to the complex behavior of the loops being placed on one of their side. The investigated structures not also have unclassified complexity but also have some links which have more than three joints (Figure 2.19).

Besides using the frieze patterns, it is also possible to connect the short and long diagonals of a loop to obtain a pattern on a curve. Using two different connection types, different linkages are obtained (Figure 2.20).
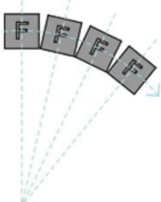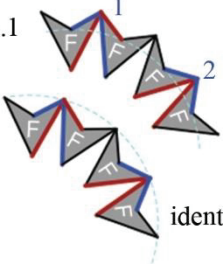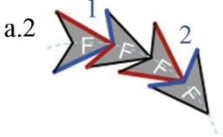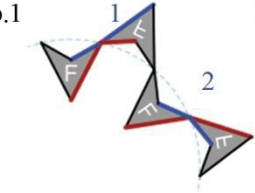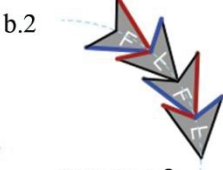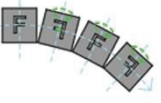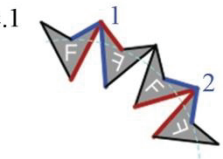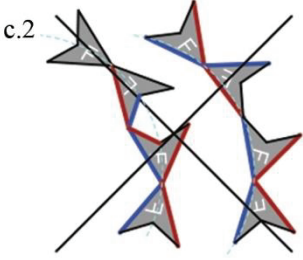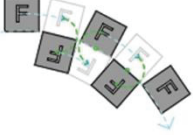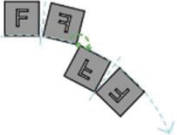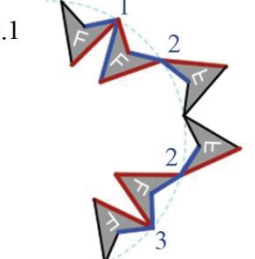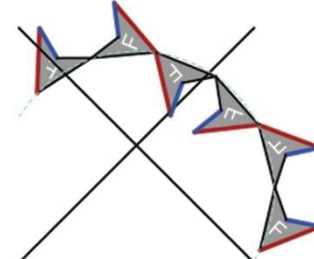
PATTERN TYPE	ON CURVE
a. HOP (F1)	a.1 a.2 identical with a.1
b. STEP (F2)	b.1 b.2 same as a.2
c. SIDLE (F3)	c.1 c.2 same as a.1
d. DIZZY SIDLE (F4)	d.1 same as b.1 d.2 same as a.2
e. DIZZY JUMP (F5)	e.1

Figure 2.16. Dart Loop Frieze Patterns
(Source: Yar, 2018)
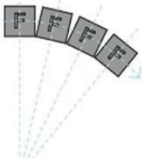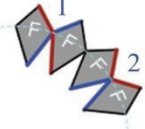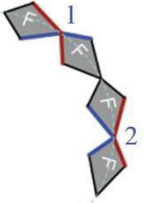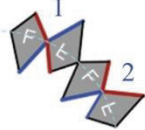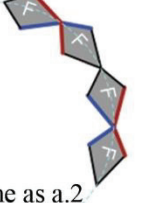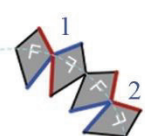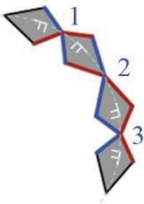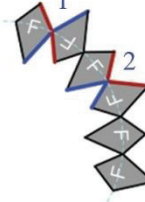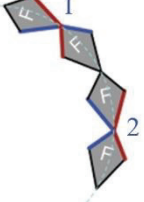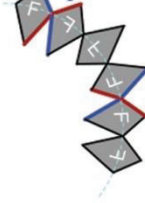
PATTERN TYPE	ON CURVE		SPECIAL CASES
a. HOP (F1)	a.1	a.2	Polar Unit
b. STEP (F2)	b.1	b.2 same as a.2	
c. SIDLE (F3)	c.1 same as a.2	c.2	
d. DIZZY SIDLE (F4)	d.1	d.2	
e. DIZZY JUMP (F5)	e.1		

Figure 2.17. Kite Loop Frieze Patterns
(Source: Yar, 2018)
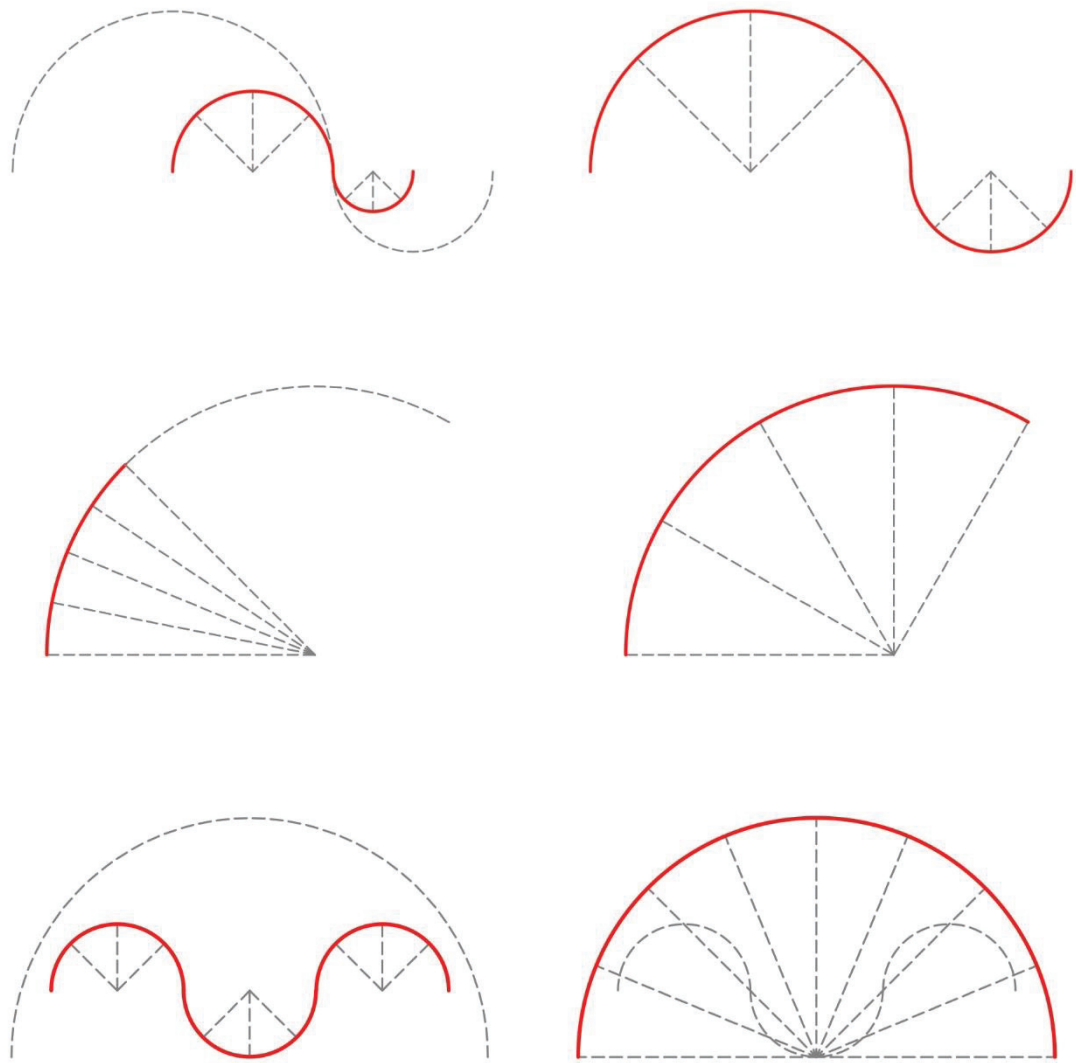
Figure 2.18. Transformation type classifications
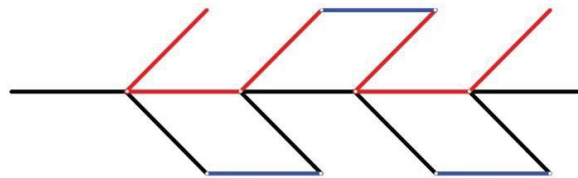
Figure 2.19. Quaternary links (black) in a rhombus assembly
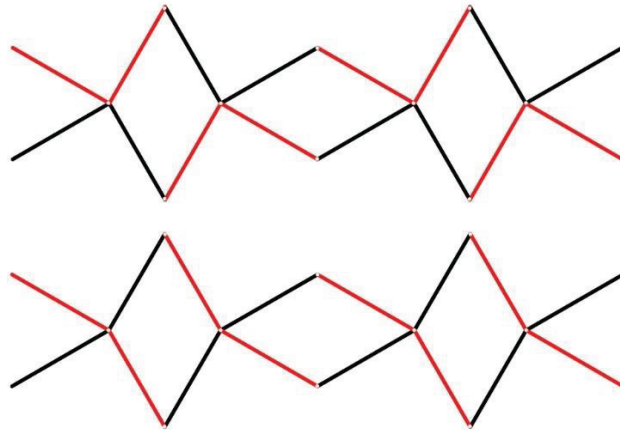
Figure 2.20. Two different linkages obtained by connecting short and long diagonals of rhombi

When a loop has vertical symmetry (Figure 2.21), Step (F2) and Dizzy Sidle (F4) patterns and Hop (F1) and Sidle (F3) patterns are indistinguishable.
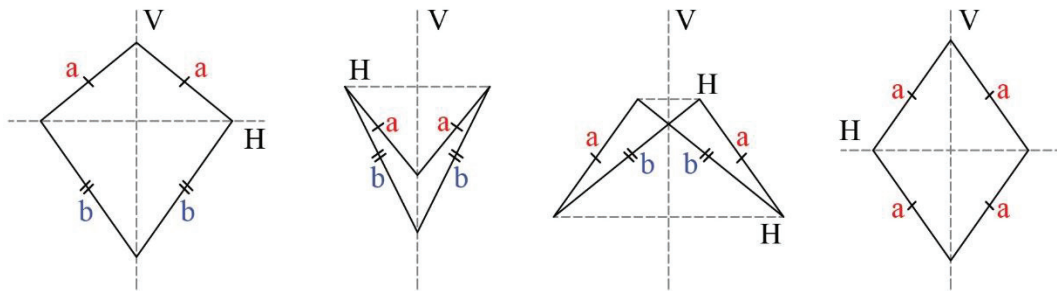
Figure 2.21. Vertical symmetric loops

By applying these various symmetry operations methods, several scissor linkages comprising different type of loops are obtained. The motions of these linkages are classified according to the change in the diagonal of the second loop (S_2) and the angle between the diagonals (α) as the diagonal of the first loop (S_1) increases (Figure 2.22).
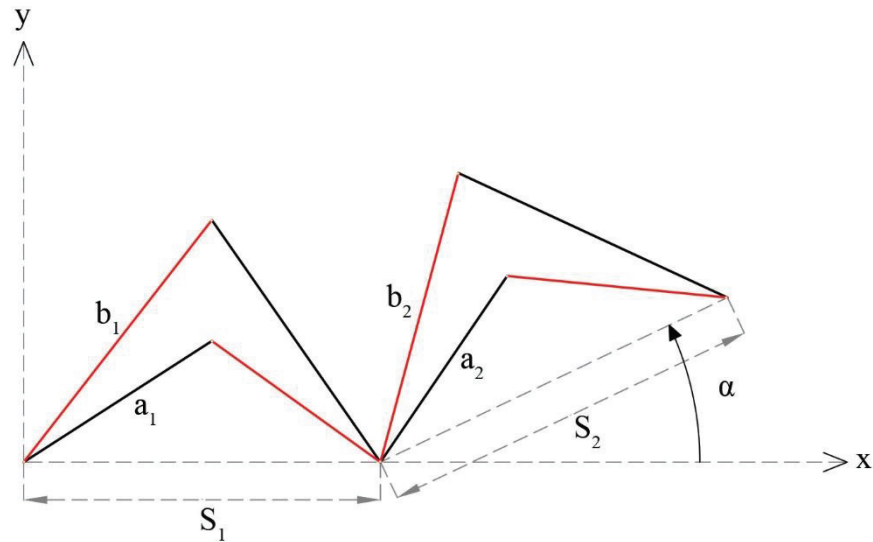
Figure 2.22. Coordinate system for the loop assemblies

Over 100 assemblies are simulated and examined using a CAD software. This analysis not only provides new assemblies, but also ideas about how to make assemblies for more complex cases. These motions can be classified under 6 types (Tables 1 and 2).

Table 1. Motion Classification

Types	Extraction			Contraction		
	S_1	S_2	α	S_1	S_2	α
Type-1	Increasing	Increasing	Increasing	Decreasing	Decreasing	Decreasing
Type-2	Increasing	Increasing	Decreasing	Decreasing	Decreasing	Increasing
Type-3	Increasing	Decreasing	Increasing	Decreasing	Increasing	Decreasing
Type-4	Increasing	Decreasing	Decreasing	Decreasing	Increasing	Increasing
Type-5	Increasing	Increasing	No Change	Decreasing	Increasing	No Change
Type-6	Increasing	Decreasing	No Change	Decreasing	Decreasing	No Change

Table 2. The number of possibilities

Types	The Number of Possibilities
Type-1	13 Assemblies
Type-2	7 Assemblies
Type-3	18 Assemblies
Type-4	6 Assemblies
Type-5	7 Assemblies
Type-6	2 Assemblies

Only one assembly of Type-2 could be used for Angular Deployment. Type 1 results in linkages with a well-structured transformable motion. Type 3 and Type-4 cannot be used for Angular or Scaling Deployment - such complex motions could just be considered in Transformability cases. However, Type-5 and Type-6 have importance since angle α does not change. Type-6 does not result in Scaling Deployment, but Type-5 does. Type-5 assemblies have Scaling Deployment ratio if the link lengths ratio is constant for all loops.

For Scaling Deployment, 7 different assemblies including same type and similar geometric dimensions with different ratio are found. The first one is the well-known rhombus assembly (Figure 2.23) (Hoberman, 1991).

The second one is with the parallelogram assemblies. During the construction, geometrically similar loops should be located on each segment (Figure 2.24). The third and fourth cases are 2 different kite assemblies. All kites should be similar. One of these assemblies is depicted in Figure 2.25 (Bai et al., 2014). The other alternative is explained in detail in a latter Section.
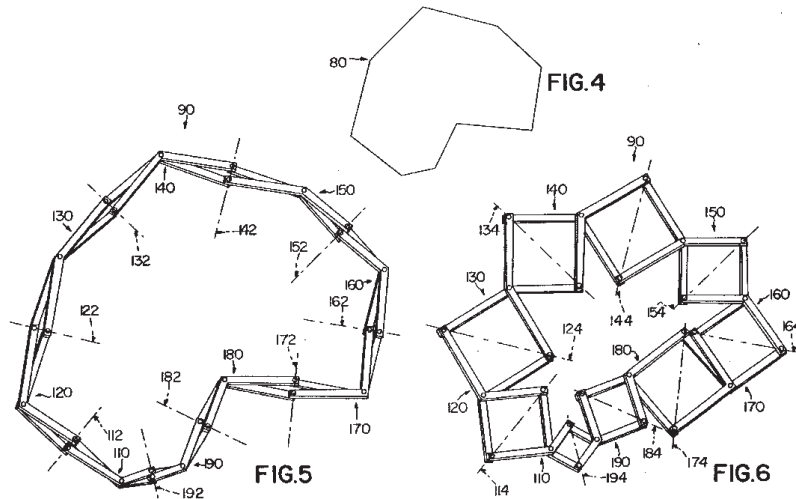
Figure 2.23. Rhombus assemblies for scaling deployment
(Source: Hoberman, 1991)
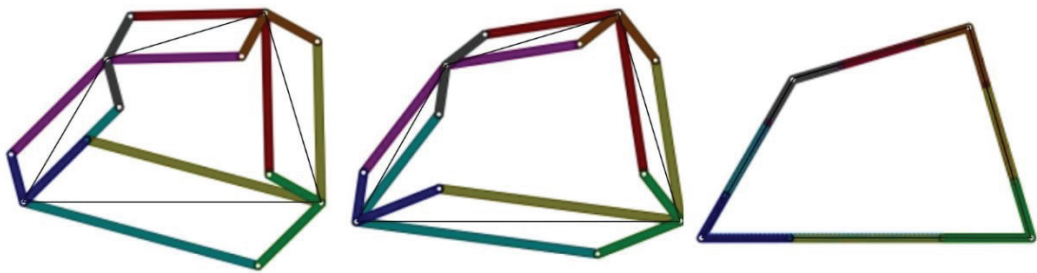
Figure 2.24. Parallelogram assemblies for scaling deployment
(Source: Bai et al., 2014)
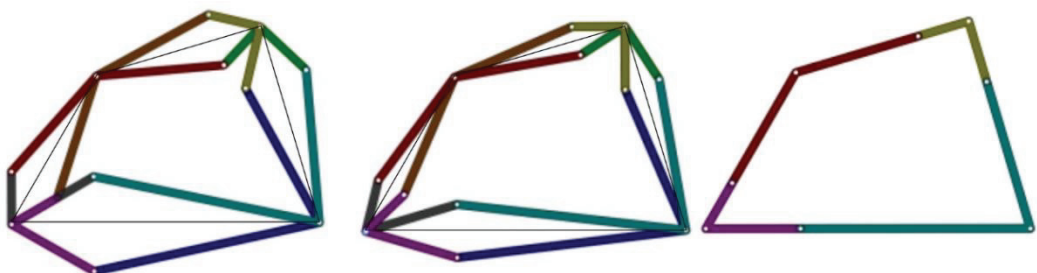
Figure 2.25. Kite assemblies for scaling deployment
(Source: Bai et al., 2014)

35

The fifth assembly is an anti-parallelograms assembly. Again, similar anti-parallelograms are used (Figure 2.26) (Gür et al., 2017, 2018).
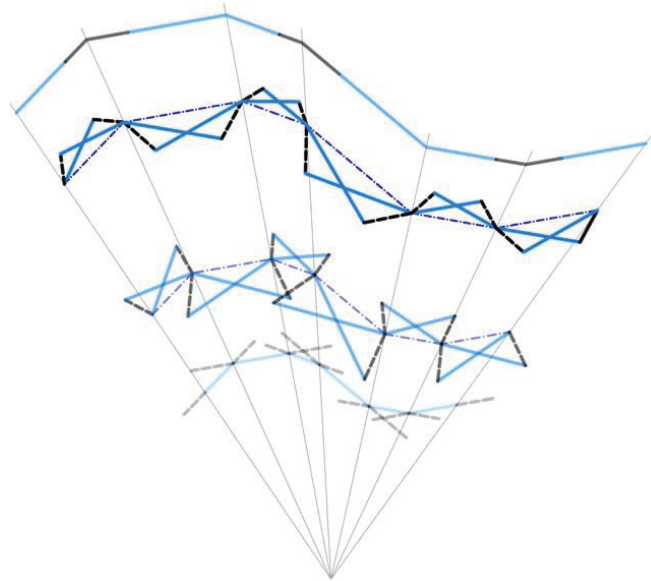
Figure 2.26. Deployment anti-parallelogram linkage on an arbitrary curve
(Source: Gür et al., 2018)

This approach introduces 2 new type scaling deployment linkages as the sixth and seventh assemblies comprising dart (Figure 2.27) and parallelogram (Figure 2.28) loops. As in the previous scaling assemblies, these assemblies also have geometrically similar loops.

For the Angular Deployment, only kite assembly can be used (Figure 2.29). The radius slightly changes during the motion, but the major change is in the angle. Also, it is possible to have the same radius in the initial and final configuration.
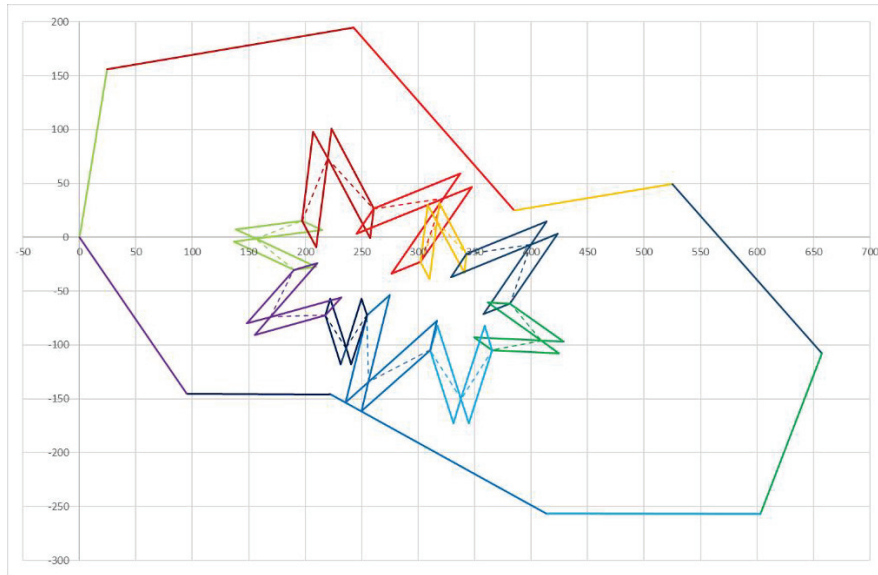
Figure 2.27. Scaling Deployment parallelogram mechanism
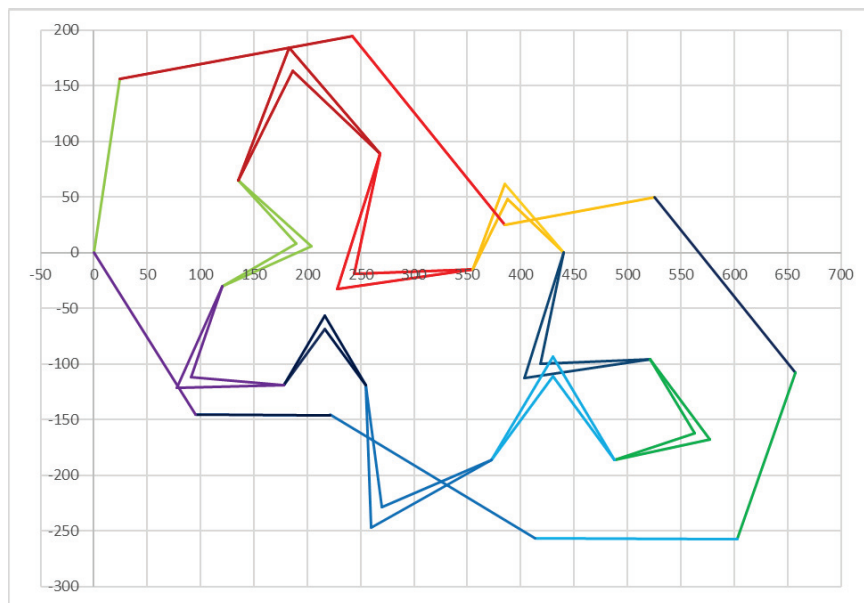
Figure 2.28. Scaling Deployment dart mechanism
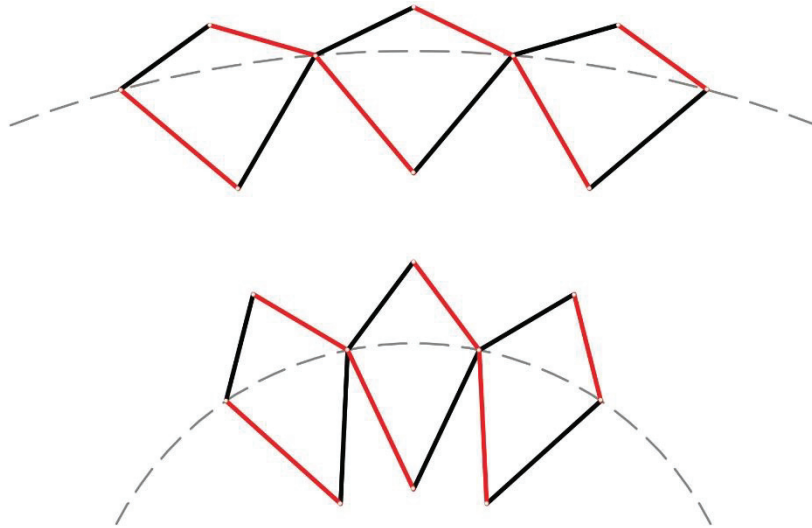
Figure 2.29. Kite angular deployment assemblies

In some dart (Figure 2.30) and anti-parallelogram (Figure 2.31) assemblies with identical loops, although the nodes remain on a circle, the radius change is extremely much, so these assemblies cannot be considered to have angular deployment.
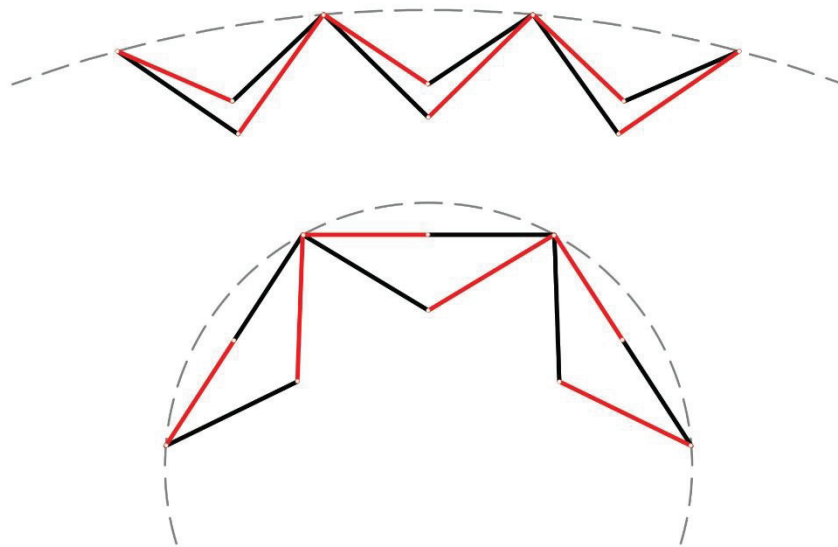
Figure 2.30. Dart angular deployment assemblies
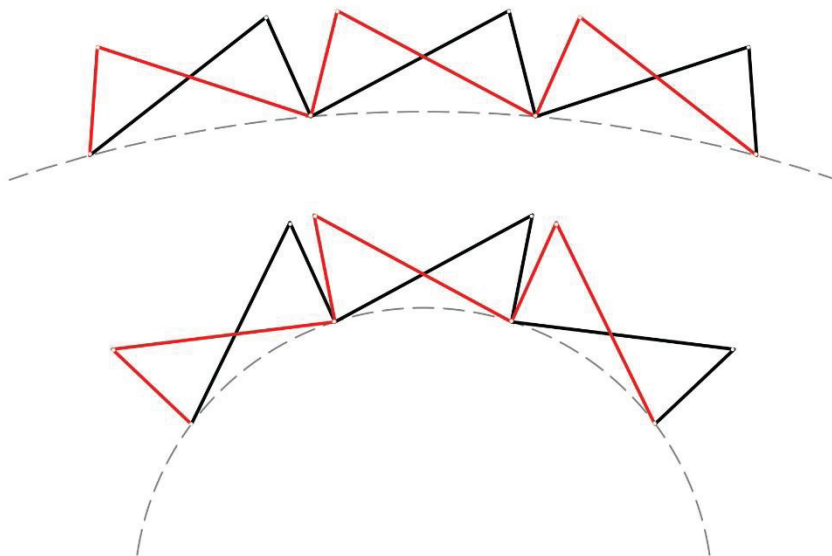
Figure 2.31. Antiparallelogram angular deployment assemblies

CHAPTER 3

DIMENSIONAL DESIGN

In this Chapter, examples for scaling deployment, angular deployment and transformability are mathematically modelled for synthesis. The given curves are discretized to polylines and dimensional design is performed.

3.1. Discretization of the Curves

The given initial and final form of the curve are discretized to n line segments. For n-line segments, there are n nodes for a closed curve and n + 1 nodes for an open curve. This discretization causes an error between the curves and the polylines. This error could be minimized. Preferably the given curves are discretized according the changing radius of curvature along the curve. The lengths between adjacent nodes are longer for larger radius. Otherwise, more are located more frequently when the radius is smaller (Figure 3.1) (Hamann et al., 1994).
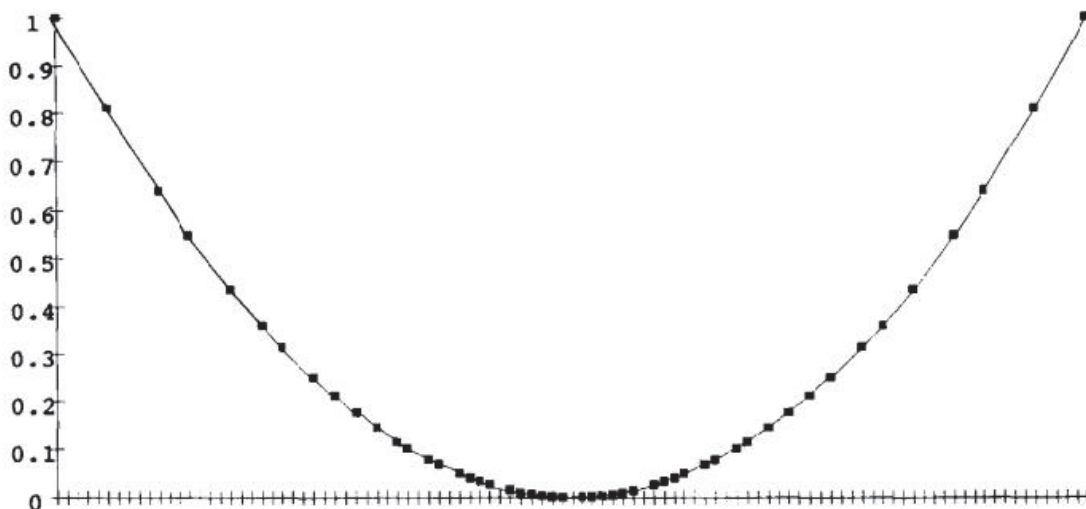
Figure 3.1. Data point selection for a selected curve
(Source: Hamann, 1994)

In scaling deployment, the lengths between nodes can change. The radius should be at least approximately constant along the path in angular deployment, so the discretization method of Hamann (1994) locates the nodes equally.

3.2. Scaling Deployable Linkages

In scaling deployment, the length of the line segments of a polyline can be presented by S_n for each segment n. Figure 3.2 illustrates an anti-parallelogram assembly, but the forthcoming formulations and discussions are valid for all type of assemblies with scaling deployment.
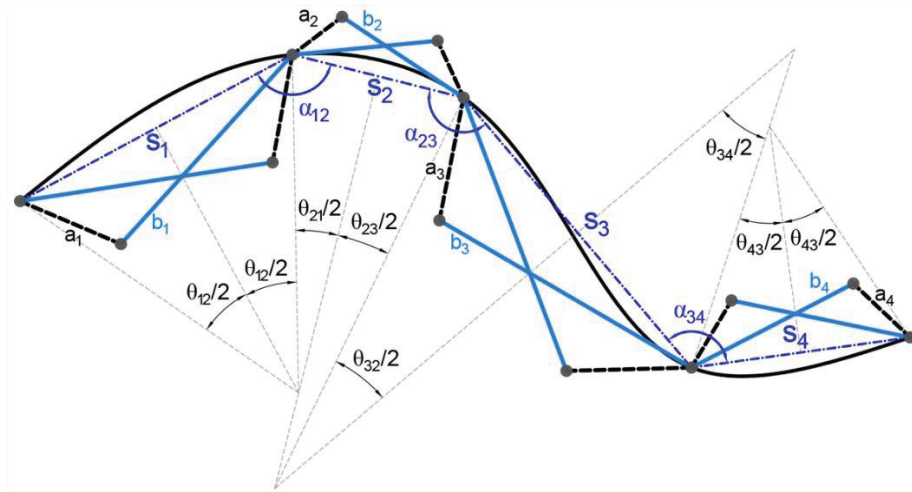
Figure 3.2. Parameters of the linkage
(Source: Gür et al., 2018)

One of the segments is selected as the primary segment. The ratio of the n_{th} segment length to the primary can be denoted as k_n:

$$\frac{S_2}{S_1} = k_2 \quad , \quad \frac{S_3}{S_1} = k_3 \quad \dots \quad \frac{S_n}{S_1} = k_n \tag{3.1}$$

In scaling deployment, all loop types except rhombus type have a short (a_1) and a long edge (b_1). The link lengths for each loop are determined using the ratio between the link length ratio R of the loop associated with the primary segment. The ratio R

should be equal for all loops on all segments. The resulting links are in Type II, i.e. similar GAEs:

$$R = \frac{b_1}{a_1} = \frac{b_2}{a_2} = ... = \frac{b_n}{a_n} \qquad (3.2)$$

At the fully deployed form, the sum of the link lengths $(a_i + b_i)$ is equal to segment

lengths. The kink angle $\alpha_{i,i+1}$ of an angulated SLE meeting at the vertex of a polyline is simply the angle between the segments meeting at the vertex. The kink angle at a vertex is supplementary of the summation of halves of subtended angles of the neighboring segments: $\alpha_{i,i+1} + (\theta_{i,i+1} + \theta_{i+1,i})/2 = 180°$ in Figure 3.2. Since the kink angles of a pair of angulated SLEs meeting at a vertex are equal to each other, all loops deploy with the same ratio during the motion, hence resulting in a scaling linkage.

Maximum deployed to compact form ratio can be found for all scaling deployment assemblies. These ratios depend on which loop assembly is preferred. These ratios can be found for the anti-parallelogram assembly, one of the kite assemblies and both parallelogram assemblies as

$$\text{Compactness ratio: } 100 \times \frac{b_n - a_n}{b_n + a_n} = 100 \times \frac{R-1}{R+1} \qquad (3.3)$$

When the other scaling deployment assemblies are fully deployed, these ratios are zero neglecting the link length collisions. The ratio R and compactness ratio can be utilized as design measures. Once the link lengths are decided, kinematic analysis of the resulting linkage can be performed. Derivation of the kinematic analysis formulations are straightforward (see for ex. (Söylemez, 2008)). The formulations are implemented in Microsoft Office Excel (Figures 3.3-6).

	Vector₁		Vector₂		Cos(α)	α								βₙ	
	X-Coord.	Y-Coord.	X-Coord.	Y-Coord.		radian	degree		n	Sₙ	kₙ	aₙ	bₙ	rad	deg
	0,155631	0,987815	0,984808	0,173648	0,324799	1,239997	71,04658		1	158,1138	1	31,62276	126,491	1,41453	81,0466
	0,984808	0,173648	0,642788	-0,76604	0,5	1,047197	59,99998		2	221,3594	1,4	44,27187	177,0875	0,174533	10,00002
	0,642788	-0,76604	0,984808	0,173644	0,500004	1,047193	59,99975		3	221,3592	1,399999	44,27184	177,0873	-0,87266	-50
	0,984808	0,173644	0,642789	-0,76604	0,500004	1,047192	59,99971		4	142,3024	0,9	28,46048	113,8419	0,174529	9,999782
	0,642789	-0,76604	-0,34202	-0,93969	0,499999	1,047199	60,00009		5	205,5476	1,299999	41,10953	164,4381	-0,87266	-49,9999
	-0,34202	-0,93969	-1	0,000347	0,341694	1,222077	70,01988		6	158,115	1,000008	31,623	126,492	-1,91986	-110
	-1	0,000347	-0,86625	0,499604	0,866427	0,522795	29,95394		7	189,696	1,199743	37,93919	151,7568	3,141245	179,9801
	-0,86625	0,499604	-1	0,00062	0,866563	0,522522	29,93829		8	221,3632	1,400025	44,27264	177,0906	2,618451	150,0262
									9	126,3892	0,799356	25,27784	101,1114	3,140972	179,9645
									10	173,9252	1,1	34,78504	139,1402	2,150244	123,1999
									11	0	0	0	0	#DIV/0!	#DIV/0!
									12	0	0	0	0	#DIV/0!	#DIV/0!
									13	0	0	0	0	#DIV/0!	#DIV/0!
									14	0	0	0	0	#DIV/0!	#DIV/0!

Ratio (b/a) 4

	Design Points			Max	Ratio (%)	s*	cos(γ)	cos(γ+φ)	γ rad	deg	φ rad	deg
	Point No	X-Coord.	Y-Coord.	60	70	110,6797	0,973214	-0,39286	0,231975	13,29118	1,742558	99,84122
	1	0	0									
	2	24,60743	156,1872									
	3	242,6038	194,6259									
	4	384,8909	25,05505									
	5	525,0315	49,76507									
	6	657,1552	-107,693									
	7	603,0766	-256,273									
	8	413,3807	-256,207									
	9	221,624	-145,613									
	10	95,23479	-145,535									
	11	0	0									
	12	0	0									
	13	0	0									
	14	0	0									
	15	0	0									

	n	Pₙ		Pₙ₁		Pₙ₂		Pₙ₊₁	
		X-Coord.	Y-Coord.	X-Coord.	Y-Coord.	X-Coord.	Y-Coord.	X-Coord.	Y-Coord.
1	1	0	0	-30,6594	-7,74606	-9,5673	126,1287	17,2252	109,3311
-1	2	17,2252	109,3311	7,166553	66,217	194,0206	99,16446	169,8227	136,2382
1	3	169,8227	136,2382	189,8304	175,731	311,7908	30,38453	269,4236	17,53854
-1	4	269,4236	17,53854	262,9572	-10,1776	383,0778	11,0024	367,522	34,83555
1	5	367,522	34,83555	386,1006	71,50746	499,3495	-63,4569	460,0086	-75,3854
-1	6	460,0086	-75,3854	436,9309	-53,7651	390,5779	-181,119	422,1536	-179,391
1	7	422,1536	-179,391	437,0462	-214,285	274,4497	-214,229	289,3665	-179,345
-1	8	289,3665	-179,345	324,7735	-152,767	160,4106	-57,9717	155,1368	-101,929
1	9	155,1368	-101,929	165,0529	-125,181	56,71935	-125,114	66,66435	-101,874
-1	10	66,66435	-101,874	100,9138	-95,7935	19,28397	28,95043	0	0
1	11	0	0	#DIV/0!	#DIV/0!	#DIV/0!	#DIV/0!	#DIV/0!	#DIV/0!
-1	12	#DIV/0!	#DIV/0!	#DIV/0!	#DIV/0!	#DIV/0!	#DIV/0!	#DIV/0!	#DIV/0!
1	13	#DIV/0!	#DIV/0!	#DIV/0!	#DIV/0!	#DIV/0!	#DIV/0!	#DIV/0!	#DIV/0!
-1	14	#DIV/0!	#DIV/0!	#DIV/0!	#DIV/0!	#DIV/0!	#DIV/0!	#DIV/0!	#DIV/0!

Figure 3.3. Kinematic Analysis in Excel
(Source: Gür et al., 2018)

Figure 3.4. Deployment of an antiparallelogram linkages
(Source: Gür et al., 2018)

Figure 3.5. Deployment of a parallelogram linkages

Figure 3.6. Deployment of a dart linkages

3.3. Angular Deployable Linkages

In general, angular deployable linkage is designed for the angular deployment from an arbitrary initial angle to another with minimum possible radius change. Although this linkage is classically designed by assembling polar scissor units, it can also be designed using kite assemblies such that the links will not be angulated. In this Section, the dimensional design of angular deployable linkages is presented for given number of loops (n), span length (2R) and the wall thickness (t) in the deployed configuration. (Figure 3.7).
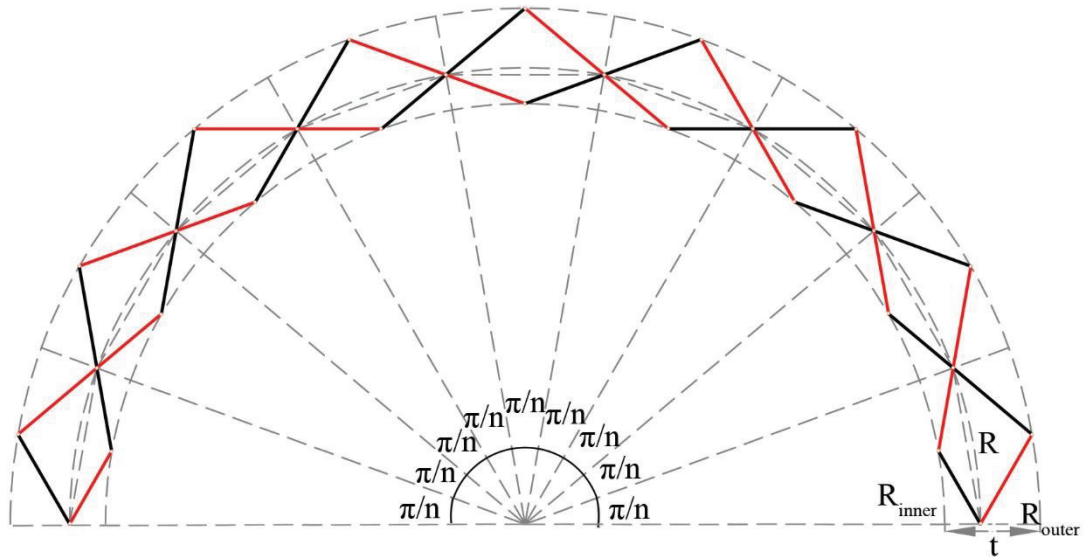
Figure 3.7. Design inputs for angular deployment mechanism

First, the circular arcs are divided into n equal segments of length S to construct an n-segmented polyline (Figure 3.8).
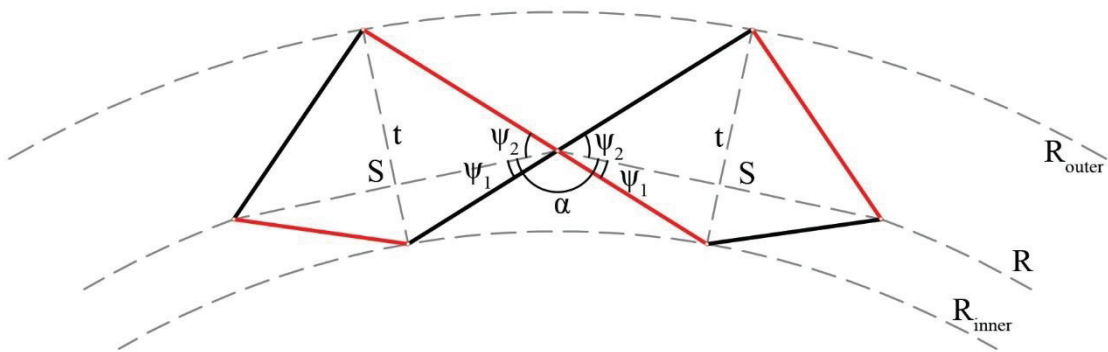
Figure 3.8. Design parameters for angular deployment mechanisms

A kink angle (α) of the polyline and number of units (n) of the loop are governed by the following equation:

$$\alpha = \pi - \frac{\pi}{n} = \frac{(n-1)\pi}{n} \tag{3.4}$$

To obtain collinear links, the summation of following angles can be written:

$$\alpha - \psi_1 + \psi_2 = \pi \quad \Rightarrow \quad \psi_2 = \pi - \alpha + \psi_1 = \psi_1 + \frac{\pi}{n} \qquad (3.5)$$

The length of a line segment of a polyline at deployed configuration can be found for each segment:

$$S = 2R \sin \frac{\pi}{2n} \qquad (3.6)$$

From the geometry, the design parameters thickness (t) can be expressed:

$$t = \frac{S}{2}\left(\tan \psi_2 + \tan \psi_1\right) \qquad (3.7)$$

Using trigonometric identities, the following expression can be found such as:

$$\frac{2t}{S} = \frac{\sin(2\psi_1 - \alpha)}{\cos \psi_1 \cos(\psi_1 - \alpha)} \qquad (3.8)$$

Using tangent of the half-angle substitution $v = \tan(\psi_1/2)$:

$$\frac{4\,v(1-v^2)\cos\alpha - \left[(1-v^2)^2 - 4\,v^2\right]\sin\alpha}{(1-v^2)\left[(1-v^2)\cos\alpha + 2\,v\sin\alpha\right]} = \frac{2t}{S} \qquad (3.9)$$

Equation 3.9 is a 4th order polynomial equation which can be solved analytically:

$$Av^4 + Bv^3 + Cv^2 + Dv + E = 0 \qquad (3.10)$$

where $\quad A = \dfrac{2t}{S}\cos\alpha + \sin\alpha, \quad B = 4\cos\alpha - \dfrac{4t}{S}\sin\alpha, \quad C = -\dfrac{4t}{S}\cos\alpha - 6\sin\alpha,$

$D = \dfrac{4t}{S}\sin\alpha - 4\cos\alpha$ and $E = \dfrac{2t}{S}\cos\alpha + \sin\alpha$. The lengths of the short (a) and long (b)

links can be expressed as:

$$a = \frac{S}{2\cos \psi_1}$$
$$b = \frac{S}{2\cos \psi_2} \qquad (3.11)$$

The inner and outer radius could be found as following:

$$R_{\text{outer}} = R\left[\cos \frac{\pi}{2n} + \sin \frac{\pi}{2n} \tan \psi_2\right]$$
$$R_{\text{inner}} = R\left[\cos \frac{\pi}{2n} - \sin \frac{\pi}{2n} \tan \psi_1\right] \qquad (3.12)$$

As an example, the angular deployment linkage for the parameters in Tables 3-6 can be seen in Figure 3.9.

Table 3. Angular deployment inputs

Inputs		
Given radius	R	120
# of segments	n	15
Thickness	t	50

Table 4. Coefficient of equation

Coefficient of Equation				
A	B	C	D	E
-3.691	-5.570	6.551	5.570	-3.691

Table 5. Roots of the equations

Solution			
v_1	v_2	v_3	v_4
0.533	0.920	-1.088	-1.875

Table 6. Results for the root v_1

Results	
ψ_1	0,980
ψ_2	1,190
R_{outer}	150,636
R_{inner}	100,636
a	22,523
b	33,713
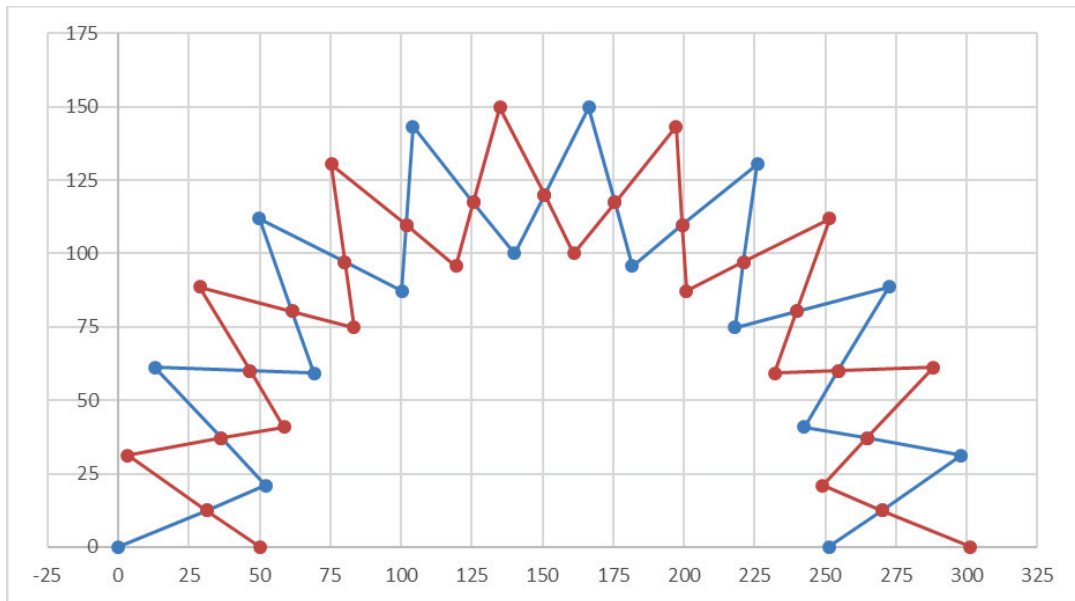
Figure 3.9. Kinematic Analysis in Excel

3.4. Transformable Linkages – Case Studies

The transformable linkages are designed for the transformation from an initial curve to some other curve with a different form. The transformable linkages noted in the literature generally require either nonsymmetrical loops or composition of different types of loops (see (Rippmann, 2007); (Zhang et al., 2016)). Since the scope of this thesis is on modular design of scissor linkages, only the transformable linkages with the same type of loops are analyzed. Various such modular designs can be constructed and the dimensional design of each and every type is different. In this Section, the dimensional designs of three selected transformable linkages are presented as case studies. The selected type of transformation for all three linkages is in between two circular arcs with different radii and subtended angles. It is assumed that the curve form remains as a circular arc at any configuration during the motion of the linkage.

First, the circular arcs are segmented into n equal segments to construct an n-segmented polyline. The length of a line segment of a polyline at an arbitrary configuration can be presented by S for each segment (Figure 3.10). S changes during the motion. Let $S = S_1$ at the initial form and $S = S_2$ at the final form.

49
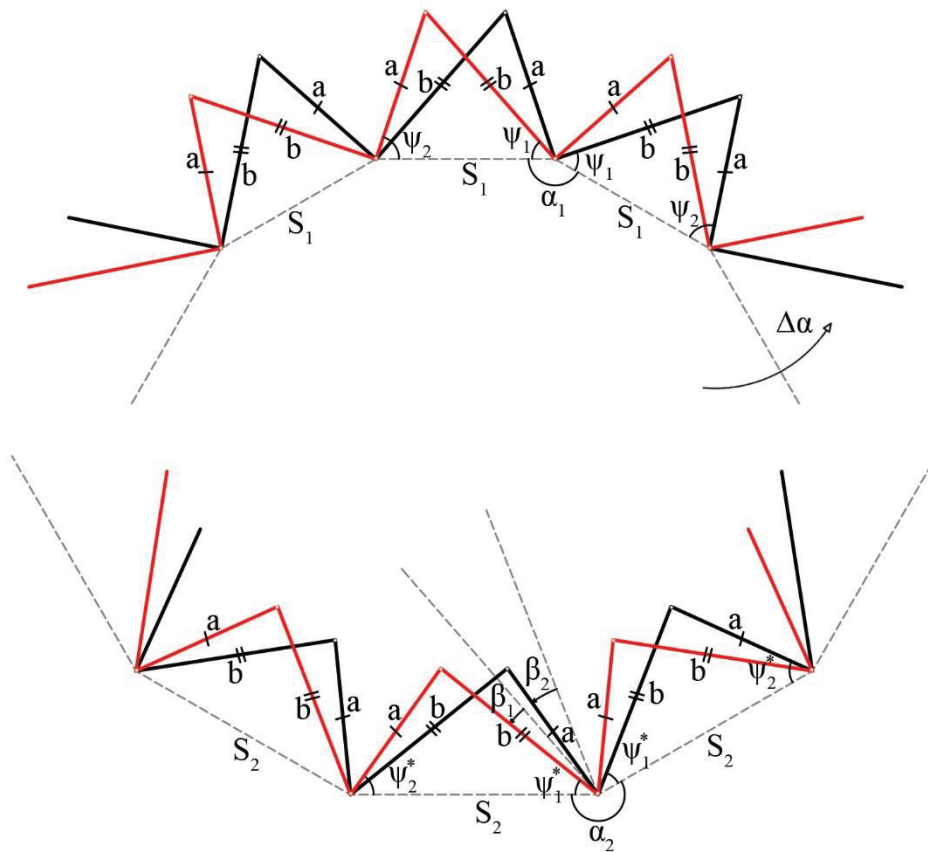
Figure 3.10. Parameter of the linkages for the anti-parallelogram assembly

The angular change $\Delta\alpha = \alpha_2 - \alpha_1$ of segmented poly-line is assumed as given. All loop types except the rhombus have a short (a) and a long side (b). The link lengths of this type of loops are determined using the link length ratios. For identical line segments, the ratio R should be equal for all loops:

$$R = \frac{b}{a} \tag{3.13}$$

The ratio μ of initial segment length to the final segment length could be defined as:

$$\mu = \frac{S_1}{S_2} \tag{3.14}$$

The compact and deployed form of the anti-parallelogram assembly are illustrated in Figure 3.10. The parameters of a loop in compact form S_1, ψ_1, ψ_2 and in deployed form S_2, ψ_1^*, ψ_2^* are governed by the following equations:

$$\frac{a}{\sin \psi_1} = \frac{b}{\sin \psi_2} = \frac{S_1}{\sin(\psi_1 + \psi_2)}$$
$$\frac{a}{\sin \psi_1^*} = \frac{b}{\sin \psi_2^*} = \frac{S_2}{\sin(\psi_1^* + \psi_2^*)}$$

(3.15)

Therefore

$$a = \frac{S_1 \sin \psi_1}{\sin(\psi_1 + \psi_2)} = \frac{S_2 \sin \psi_1^*}{\sin(\psi_1^* + \psi_2^*)}$$
$$b = \frac{S_1 \sin \psi_1}{\sin(\psi_1 + \psi_2)} = \frac{S_2 \sin \psi_2^*}{\sin(\psi_1^* + \psi_2^*)}$$

(3.16)

ψ_1, ψ_2, ψ_1^*, ψ_2^* angles can be represented in the following forms:

$$\psi_1^* = \mathrm{acos}\left(\frac{S_2^2 + b^2 - a^2}{2bS_2}\right)$$
$$\psi_2^* = \mathrm{acos}\left(\frac{S_2^2 + a^2 - b^2}{2aS_2}\right)$$
$$\psi_1 = \mathrm{acos}\left(\frac{S_1^2 + b^2 - a^2}{2bS_1}\right)$$
$$\psi_2 = \mathrm{acos}\left(\frac{S_1^2 + a^2 - b^2}{2aS_1}\right)$$

(3.17)

Since all loops are identical, the parameter ψ_1^*, ψ_2^* can be presented with Equation 3.18, where β_1 and β_2 are the amount of rotation of the links from initial to final configuration.

$$\psi_1^* = \psi_1 + \beta_2 - \Delta\alpha = \psi_1 - \beta_1$$
$$\psi_2^* = \psi_2 + \beta_1 - \Delta\alpha = \psi_2 - \beta_2$$

(3.18)

from which β_1 and β_2 are found as:

$$\beta_1 = \psi_1 - \psi_1^* = \psi_2^* - \psi_2 + \Delta\alpha$$
$$\beta_2 = \psi_2 - \psi_2^* = \psi_1^* - \psi_1 + \Delta\alpha$$

(3.19)

In terms of equations above $\Delta\alpha$ can be expressed as:

$$\Delta\alpha = \beta_1 + \beta_2 = \psi_1 - \psi_1^* + \psi_2 - \psi_2^*$$

(3.20)

Using Equation 3.17 and 3.20 $\Delta\alpha$ can be derived as

$$\Delta\alpha = \mathrm{acos}\left(\frac{S_1^2 + b^2 - a^2}{2bS_1}\right) + \mathrm{acos}\left(\frac{S_1^2 + a^2 - b^2}{2aS_1}\right) - \psi_1^* - \psi_2^*$$

(3.21)

Assuming that at fully deployed form the links are on the polyline, $\psi_1^* = \psi_2^* = 0$, $a + b = (1 + R)a = S_2$ and the kink angle of the angulated SLEs are equal to $2\pi - \alpha_2$. Then Equation 3.21 becomes

$$\Delta\alpha = \mathrm{acos}\left(\frac{\mu^2(1+R)^2 + R^2 - 1}{2\mu R(1+R)}\right) + \mathrm{acos}\left(\frac{\mu^2(1+R)^2 + 1 - R^2}{2\mu(1+R)}\right) = \psi_1 + \psi_2 \quad (3.22)$$

In Equation 3.22, μ and $\Delta\alpha$ are known from the initial and final curve forms, hence R can be calculated using Equation 3.23.

$$S_1^2 = a^2 + b^2 + 2ab\cos(\Delta\alpha) \quad (3.23)$$

Equation 3.23 can be rearranged as

$$\mu^2(R+1)^2 a^2 = (R^2+1)a^2 + 2Ra^2\cos(\Delta\alpha) \quad (3.24)$$

Rearranging Equation 3.24, Equation 3.25 can be written as

$$R^2(1-\mu^2) + 2R(\cos(\Delta\alpha) - \mu^2) + (1-\mu^2) = 0 \quad (3.25)$$

Because of the two different solutions are reciprocals of each other, the only solution can be written as:

$$1 < R = \frac{-\cos(\Delta\alpha) + \mu^2 + \sqrt{(\cos(\Delta\alpha) - \mu^2)^2 - (1-\mu^2)^2}}{1-\mu^2} \leq \frac{1+\mu}{1-\mu} \quad (3.26)$$

Once R is determined, a and b can be solved as

$$a = \frac{S_2}{1+R} \quad \text{and} \quad b = Ra \quad (3.27)$$

The limit of Equation 3.22, as R goes to $\dfrac{1+\mu}{1-\mu}$, is found as in Equation 3.29 when the loop reaches it's the deployed form.

$$\lim_{R \to \frac{1+\mu}{1-\mu}} \Delta\alpha = 2\mathrm{acos}(-1) = \pi \quad (3.29)$$

The limit of Equation 3.22, as R goes to 1, is found as in Equation 3.30 when the loop is at it's the compact form.

$$\lim_{R \to 1} \Delta\alpha = 2\mathrm{acos}(\mu) \quad (3.30)$$

Figure 3.11. Parameters of the linkages for dart assembly

The compact and deployed forms of the dart loop assembly are illustrated in Figure 3.11. The parameters of the loop in compact form S_1, ψ_1, ψ_2 and in deployed form S_2, ψ_1^*, ψ_2^* are governed by the following equations:

$$2\cos\psi_1 a = 2\cos\psi_2 b = S_1$$
$$2\cos\psi_1^* a = 2\cos\psi_2^* b = S_2 \tag{3.31}$$

where

$$a = \frac{S_1}{2\cos\psi_1} = \frac{S_2}{2\cos\psi_1^*}$$
$$b = \frac{S_1}{2\cos\psi_2} = \frac{S_2}{2\cos\psi_2^*} \tag{3.32}$$

ψ_1, ψ_2, ψ_1^*, ψ_2^* angles can be represented in the following forms:

$$\psi_1^* = \mathrm{acos}\left(\frac{S_2}{2a}\right)$$

$$\psi_2^* = \mathrm{acos}\left(\frac{S_2}{2b}\right)$$

$$\psi_1 = \mathrm{acos}\left(\frac{S_1}{2a}\right)$$

(3.33)

$$\psi_2 = \mathrm{acos}\left(\frac{S_1}{2b}\right)$$

Because of the link connection, the parameter ψ_1^* can be presented with Equation 3.34 where $\Delta\alpha$ is the change in the king angle of the polylines.

$$\psi_1^* = \psi_1 + \beta_2 - \Delta\alpha = \psi_1 - \beta_1$$
$$\psi_2^* = \psi_2 + \beta_1 - \Delta\alpha = \psi_2 - \beta_2$$

(3.34)

where β_1 and β_2 can be found as:

$$\beta_1 = \psi_1 - \psi_1^* = \psi_2^* - \psi_2 + \Delta\alpha$$
$$\beta_2 = \psi_2 - \psi_2^* = \psi_1^* - \psi_1 + \Delta\alpha$$

(3.35)

In terms of equations above $\Delta\alpha$ can be expressed as:

$$\Delta\alpha = \beta_1 + \beta_2$$
$$\Delta\alpha = \psi_1 + \psi_2 - \psi_1^* - \psi_2^*$$

(3.36)

Equation 3.33 can be rearranged as

$$\cos\left(\psi_1^*\right) = \frac{S_2}{2a} = \frac{S_2}{2a} = \frac{2a}{2a} = 1$$

$$\cos\left(\psi_2^*\right) = \frac{S_2}{2b} = \frac{S_2}{2b} = \frac{2a}{2aR} = \frac{1}{R}$$

$$\cos\left(\psi_1\right) = \frac{S_1}{2a} = \frac{\mu S_2}{2a} = \frac{2\mu a}{2a} = \mu$$

(3.37)

$$\cos\left(\psi_2\right) = \frac{S_1}{2b} = \frac{\mu S_2}{2b} = \frac{2\mu a}{2aR} = \frac{\mu}{R}$$

Assuming that at fully deployed form the links are on the polyline, $\psi_1^* = 0$, $S_2 = 2a$ and the kink angle of the angulated SLEs are equal to $2\pi - \alpha_2$. Then Equation 3.36 becomes

$$\Delta\alpha = \psi_1 + \psi_2 - \psi_2^*$$
$$\psi_2 = \Delta\alpha - \psi_1 + \psi_2^*$$

(3.38)

$$\cos\left(\psi_2\right) = \cos\left(\Delta\alpha - \mathrm{acos}\mu + \mathrm{acos}\left(\frac{1}{R}\right)\right)$$

54

Using trigonometric identities Equation 3.38 can be rearranged as

$$\frac{\mu}{R} = \frac{\cos(\Delta\alpha - a\cos\mu)}{R} - \sin(\Delta\alpha - a\cos\mu)\frac{\sqrt{R^2 - 1}}{R} \qquad (3.39)$$

Solving for R in Equation 3.39, the only solution can be written as:

$$R = \frac{\sqrt{1 - 2\mu\cos(\Delta\alpha - a\cos\mu) + \mu^2}}{\sin(\Delta\alpha - a\cos\mu)} \qquad (3.40)$$

The limit of Equation 3.36, as R goes to infinity, is found as in Equation 3.41 when the loop reaches its deployed form.

$$\lim_{R\to\infty} \Delta\alpha = a\cos(\mu) + a\cos(0) - a\cos(0) = a\cos(\mu) \qquad (3.41)$$

The limit of Equation 3.36, as R goes to 1, is found as in Equation 3.42 when the loop is at its compact form.

$$\lim_{R\to1} \Delta\alpha = a\cos(\mu) + a\cos(\mu) = 2a\cos(\mu) \qquad (3.42)$$
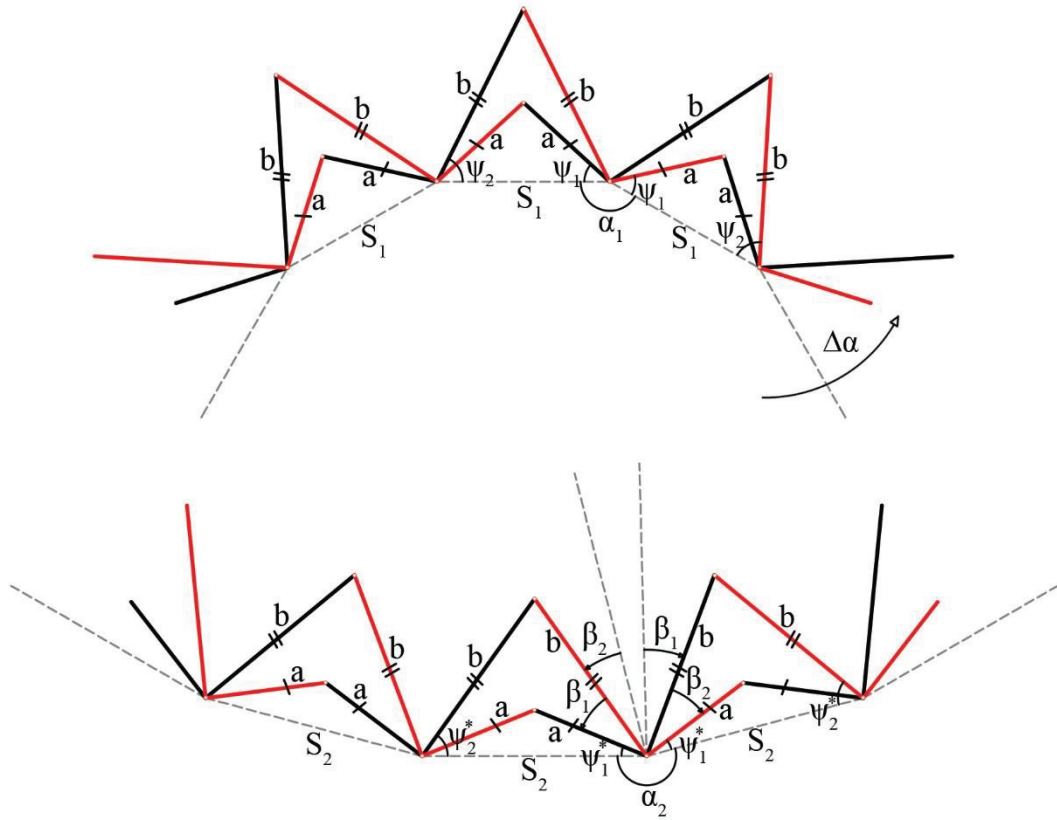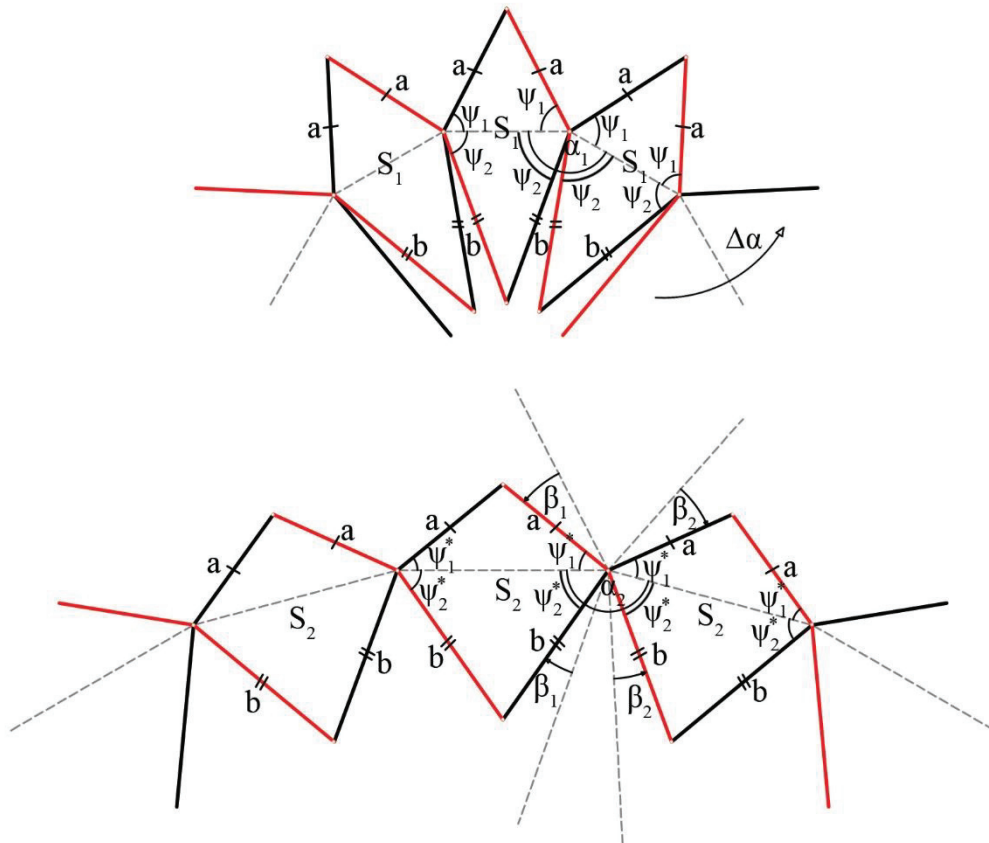

Figure 3.12. Parameters of the linkages for kite assembly

The compact and deployed forms of the kite loop assembly are illustrated in Figure 3.12. The parameters of the loop in compact form S_1, ψ_1, ψ_2 and in deployed form S_2, ψ_1^*, ψ_2^* are governed by the following equations:

$$2\cos\psi_1 a = 2\cos\psi_2 b = S_1$$
$$2\cos\psi_1^* a = 2\cos\psi_2^* b = S_2$$

(3.43)

where

$$a = \frac{S_1}{2\cos\psi_1} = \frac{S_2}{2\cos\psi_1^*}$$
$$b = \frac{S_1}{2\cos\psi_2} = \frac{S_2}{2\cos\psi_2^*}$$

(3.44)

ψ_1, ψ_2, ψ_1^*, ψ_2^* angles can be represented in the following forms:

$$\psi_1^* = \mathrm{acos}\left(\frac{S_2}{2a}\right)$$
$$\psi_2^* = \mathrm{acos}\left(\frac{S_2}{2b}\right)$$
$$\psi_1 = \mathrm{acos}\left(\frac{S_1}{2a}\right)$$
$$\psi_2 = \mathrm{acos}\left(\frac{S_1}{2b}\right)$$

(3.45)

Because of the link connection, the parameter ψ_1^* can be presented with Equation 3.45 where $\Delta\alpha$ is the king angle.

$$\psi_1^* = \psi_1 - \beta_2 - \Delta\alpha = \psi_1 - \beta_1$$
$$\psi_2^* = \psi_2 - \beta_1 + \Delta\alpha = \psi_2 - \beta_2$$

(3.46)

where β_1 and β_2 are found as:

$$\beta_1 = \psi_1 - \psi_1^* = \psi_2 - \psi_2^* + \Delta\alpha$$
$$\beta_2 = \psi_2 - \psi_2^* = \psi_1 - \psi_1^* - \Delta\alpha$$

(3.47)

In terms of equations above $\Delta\alpha$ can be expressed as:

$$\Delta\alpha = \beta_1 - \beta_2$$
$$\Delta\alpha = \psi_1 - \psi_1^* - \psi_2 + \psi_2^*$$

(3.48)

Equation 3.45 can be rearranged as

$$\cos\left(\psi_1^*\right) = \frac{S_2}{2a} = \frac{S_2}{2a} = \frac{2a}{2a} = 1$$

$$\cos\left(\psi_2^*\right) = \frac{S_2}{2b} = \frac{S_2}{2b} = \frac{2a}{2aR} = \frac{1}{R}$$

$$\cos\left(\psi_1\right) = \frac{S_1}{2a} = \frac{\mu S_2}{2a} = \frac{2\mu a}{2a} = \mu \qquad (3.49)$$

$$\cos\left(\psi_2\right) = \frac{S_1}{2b} = \frac{\mu S_2}{2b} = \frac{2\mu a}{2aR} = \frac{\mu}{R}$$

Assuming that at fully deployed form the links are on the polyline, $\psi_1^* = 0$, $2a = S_2$ and the kink angle of the angulated SLEs are equal to $2\pi - \alpha_2$. Then Equation 3.48 becomes

$$\Delta\alpha = \psi_1 - \psi_2 + \psi_2^*$$

$$\psi_2 = \psi_1 + \psi_2^* - \Delta\alpha \qquad (3.49)$$

$$\cos\left(\psi_2\right) = \cos\left(\mathrm{acos}\mu - \Delta\alpha + \mathrm{acos}\left(\frac{1}{R}\right)\right)$$

Equation 3.49 can be rearranged as

$$\frac{\mu}{R} = \frac{\cos\left(\mathrm{acos}\mu - \Delta\alpha\right)}{R} - \sin\left(\mathrm{acos}\mu - \Delta\alpha\right)\frac{\sqrt{R^2 - 1}}{R} \qquad (3.50)$$

Solving for R in Equation 3.49, the only solution can be written as:

$$R = \frac{\sqrt{1 - 2\mu\cos\left(\mathrm{acos}\mu - \Delta\alpha\right) + \mu^2}}{\sin\left(\mathrm{acos}\mu - \Delta\alpha\right)} \qquad (3.51)$$

The limit of Equation 3.48 as R goes to infinity, is found as in Equation 3.52 when the loop reaches its deployed form.

$$\lim_{R\to\infty} \Delta\alpha = \mathrm{acos}(\mu) - \mathrm{acos}(0) + \mathrm{acos}(0) = \mathrm{acos}(\mu) \qquad (3.52)$$

The limit of Equation 3.48, as R goes to 1, is found as in Equation 3.53 when the loop is at its compact form.

$$\lim_{R\to 1} \Delta\alpha = \mathrm{acos}(\mu) - \mathrm{acos}(\mu) + \mathrm{acos}(1) = 0 \qquad (3.53)$$

The compactness ratio can be found for all transformable assemblies. For kite and dart assemblies, the theoretical compactness ratio is zero neglecting link collisions. These ratios depend on which loop assembly is preferred. These maximum compactness ratio for the anti-parallelogram loops can be found as

$$\mu = \frac{S_1}{S_2} = \frac{b-a}{b+a} = \frac{R-1}{R+1} \qquad (3.54)$$

57

Once the link lengths are calculated, kinematic analysis of the resulting linkage can be performed. Derivation of the kinematic analysis formulations are straightforward (see for ex. (Söylemez, 2008)). The formulations are implemented in Microsoft Excel.

Three cases are presented as numerical examples. Table 7 presents the design requirement parameters for three case studies with different loop assemblies. The illustrations of the case studies are depicted in Figures 3.13-15, where anti-parallelogram, dart and kite loop assemblies is transformed between two circular arc forms with different curvature characteristics. The resulting design parameters are listed in Table 8.

Table 7. Design Requirement Parameters

	Loop Type	S_1	S_2	α_1	α_2
Case 1	Antiparallelogram	80	100	135°	210°
Case 2	Dart	60	100	135°	210°
Case 3	Kite	50	100	160°	190°

Table 8. Resulting design Parameters

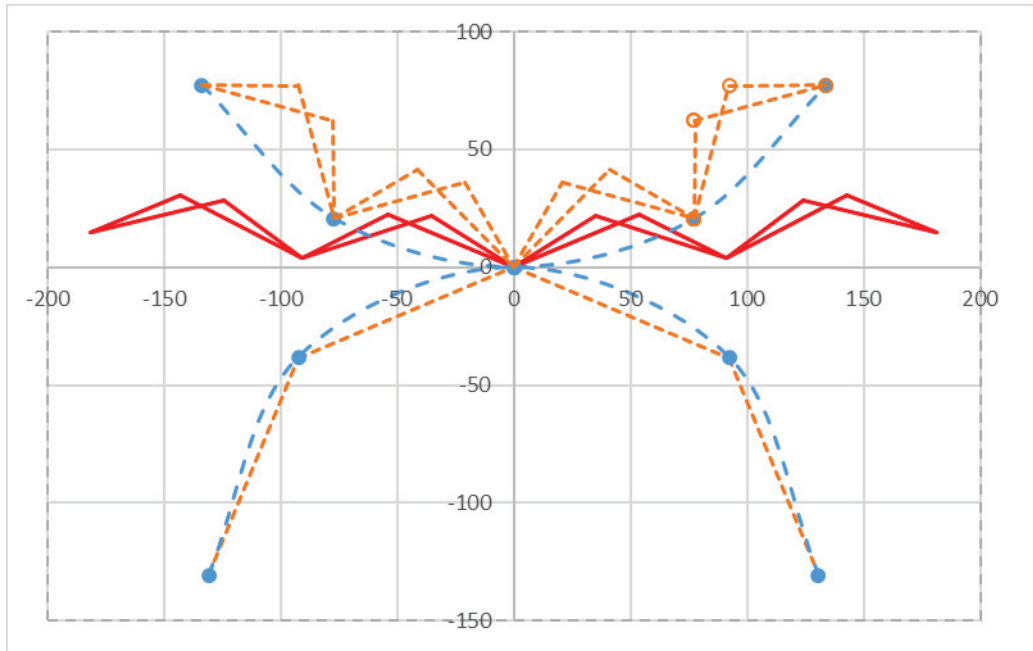|	Loop Type	R	a	b	Link Kink Angle
Case 1	Antiparallelogram	1.407	41.548	58.452	135.000°
Case 2	Dart	1.332	50.000	66.624	176.368°
Case 3	Kite	1.239	50.000	61.966	123.794°

Figure 3.13. Kinematic Analysis in Excel for antiparallelogram assembly
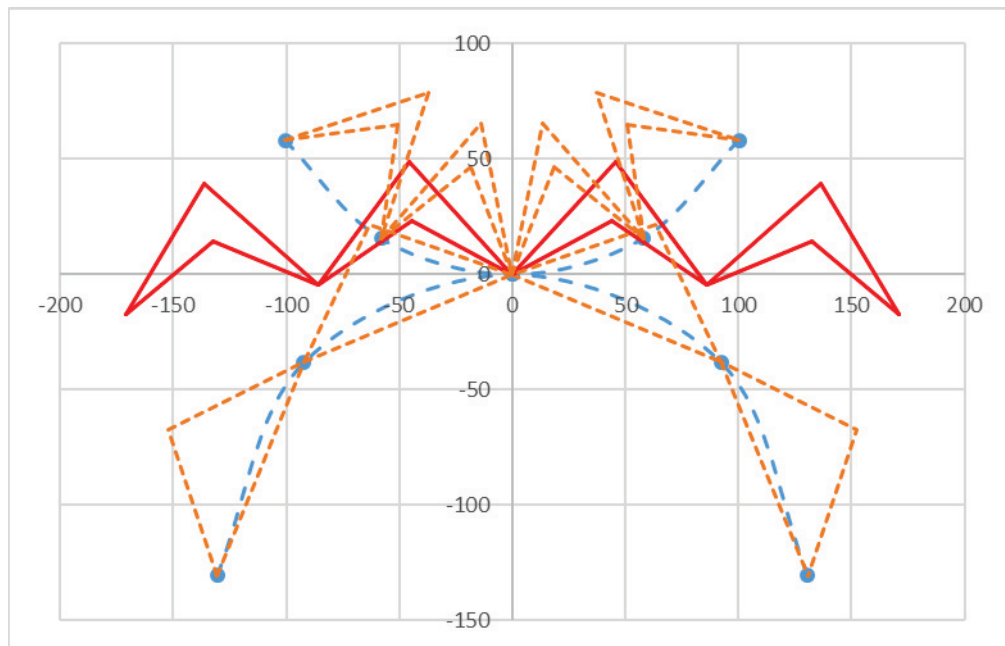

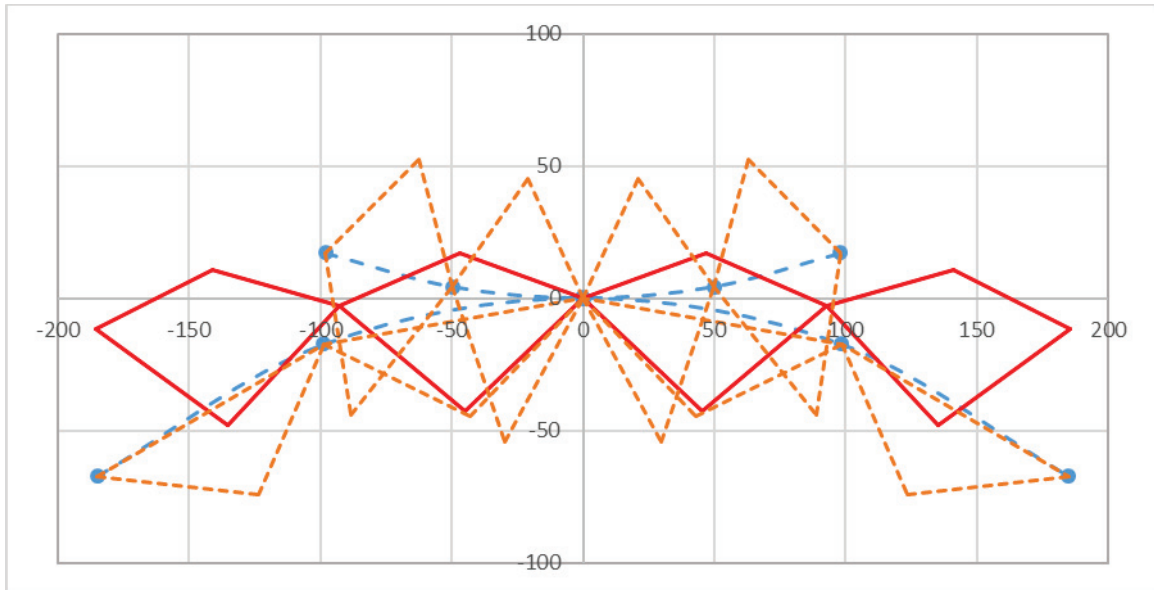Figure 3.14. Kinematic Analysis in Excel for dart assembly

Figure 3.15. Kinematic Analysis in Excel for kite assembly

CHAPTER 4

CONCLUSIONS

The aim of this thesis study is to create kinematic design methods for different scissor linkages for different motions to satisfy today's engineering structures demand. The linkages are designed for the transformation of planar curves from an initial form to a final form. The planar curves are approximated with poly-lines with nodes.

The topological alternatives of possible scissor linkages are already listed by other researchers. In order to examine the transformations these linkages are capable of, first a classification of motion characteristics of possible linkage assemblies is performed. The classification resulted in six different type of motions, some of which can lead to deployable linkages and others lead to linkages for transformable motion. The six different motion types differ by increasing/decreasing polyline segment lengths and the kink angle of adjacent segments in the poly-line. The result of this classification reveals possible type of linkages that can be used for different transformations of curves.

To perform the dimensional design of these linkages, first the given initial and final form of the approximated curve is represented by segment lengths and angles between the segments. The mathematical set of equations to design several different linkages are derived. Three assemblies for scaling deployment different from literature are analyzed and a generalized design approach for transformable assemblies are presented. Also, case studies for dimensional design are presented.

The method introduced in this study can be used as an overall guideline to design deployable structures comprising scissor linkages. The derived formulations can be implemented in a design software that can be used by architects and engineers.

As further studies, the linkages comprising different loop types should be examined to understand the behavior of their motion characteristics. The methodology in this thesis study can be used in addressing this problem as well.

REFERENCES

"AECOM - Global Maintenance Support and Services" Sprung Structures. Accessed June 27, 2018. http://www.sprung.com/case-study/aecom-global-maintenance-support-and-services/

Akgün, Yenal. *A novel transformation model for deployable scissor-hinge structures*. PhD diss., İzmir Institute of Technology, 2010.

Bai, Guochao, Shimin Wei, Duanling Li, Qizheng Liao, and Xianwen Kong. "*A Novel Synthesis Method of Polygon-Scaling Mechanisms.*" Volume 5A: 38th Mechanisms and Robotics Conference, 2014. doi:10.1115/detc2014-34934.

"Bespoke Branded Scissor Awning" Central Awnings. Last modified June 7, 2016. http://www.centralawnings.co.uk/scissor-arm-awning-bespoke-branding

Conferencistas Simposio. Accessed August 05, 2018. http://www.grupoestran.com/simposio/escringingles.html

Conway, John Horton, Heidi Burgiel, and Chaim Goodman-Strauss. *The symmetry of things*. *Wellesley, MA, A K Peters,* 2008.

Escrig, Felix. "*Expandable Space Structures.*" International Journal of Space Structures 1, no. 2 (1985): 79-91. doi:10.1177/026635118500100203.

Escrig, Felix, and Juan Pablo Valcarcel. "*Analysis of Expendable Space Bar Structures*." In IASS Symposium on Shells, Membranes, and Space Frames, 269-76. Proceedings, Osaka, Japan. Vol. 3. Elsevier Science Publishers, 1986a.

Escrig, Felix, and Juan Pablo Valcarcel. "*Great Size Umbrellas with Expendable Bar Structures.*" In The 1st International Conference on Lightweight Structures in Architecture, 676-81. Proceedings. 1986b.

Escrig, Felix, and Juan Pablo Valcarcel. "*Curved expandable space grids*." In the International Conference on the Design and Construction of Non-conventional Structures, 57-166. Proceedings, London, England. Civil-Comp Press, 1987.

Escrig, Felix, and Juan Pablo Valcarcel. "*Geometry of expandable space structures*." In the International Journal of Space Structures 8, 71-84. Proceedings. No. 1-2. 1993.

Escrig, Felix. "*General survey of deployability in architecture*." In the Second International Conference on Mobile and Rapidly Assembled Structures (MARAS 96). Proceedings, Seville, Spain. 1996.

Gantes, C. J. *Deployable Structures: Analysis and Design*. Ashurst, Southampton: WIT Press, 2001.

Gür, Şebnem. *Design of single degree-of-freedom planar linkages with antiparallelogram loops using loop assembly method*. Master's thesis, İzmir Institute of Technology, 2017.

Gür, Şebnem, Koray Korkmaz and Gökhan Kiper. "*Radially expandable ring-like structure with anti-parallelogram loops*." In the International Symposium of Mechanism and Machine Science ISMMS-2017. Proceedings, Baku, Azerbaijan. 2017.

Gür, Şebnem, Cevahir Karagöz, Gökhan Kiper, and Koray Korkmaz. "*Synthesis of Scalable Planar Scissor Linkages with Anti-Parallelogram Loops*" To be presented in: European Conference on Mechanism Science (EUCOMES 2018). Proceedings, Aachen, Germany, 2018.

Hamann, Bernd, and Jiann-Liang Chen. "*Data Point Selection for Piecewise Linear Curve Approximation*." Computer Aided Geometric Design 11, no. 3 (1994): 289-301. doi:10.1016/0167-8396(94)90004-3.

Hernández Merchan, Carlos Henrique. *Deployable structures*. PhD diss., Massachusetts Institute of Technology, 1987.

Hoberman, Charles. Reversibly expandable doubly-curved truss structure. US Patent 4,942,700, issued July 24, 1990.

Hoberman, Charles. Radial expansion/retraction truss structures. US Patent 5,024,031, issued June 18, 1991.

Hoberman, Chuck. "Mechanical Invention Through Computation - Mechanism Basics." MIT Class 6.S080 Lecture Notes, 2013, Available online at courses.csail.mit.edu/6.S080/lectures/02_all.pdf Architectural Design 102

"Hoberman Sphere", Wikipedia. Last modified March 08, 2018. https://en.wikipedia.com/Hoberman_sphere

"Hoberman Iris Dome", Google Images. Accessed June 29, 2018. https://www.google.com.tr/search?q=hoberman+%C4%B1ris+dome&source=ln ms&tbm=isch&sa=X&ved=0ahUKEwjdr7DFrfjbAhVEFiwKHYuoBpUQ_AUI CigB&biw=1536&bih=683#imgrc=NNK-mES04-YsGM:

"Hoberman Arch", Google Images. Accessed June 29, 2018. https://www.google.com.tr/search?biw=1536&bih=683&tbm=isch&sa=1&ei=he A1W7LjIISqsAHs5YaYBA&q=hoberman+arch&oq=hoberman+arch&gs_l=im g.3...0j0i8i30k1j0i24k1.82038.84484.0.84615.12.10.2.0.0.0.320.1359.2-4j1.5.0....0...1c.1.64.img...6.4.866...0i67k1j0i5i30k1.0.5C4Z52KbGe8

Illinois Engineered Products. Last modified June 14, 2016. http://www.illinoisengineeredproducts.com/iep-pair-retail-window-gate-extracted/

Kassabian, P. E., Zhong You, and Sergio Pellegrino. "*Retractable Roof Structures*." In the Institution of Civil Engineers-Structures and Buildings 134, 45-56. Proceedings. No. 1. 1999.

Kiper, Gökhan, and Eres Söylemez. "*Irregular polygonal and polyhedral linkages comprising scissor and angulated elements*." In the 1st IFToMM Asian Conference on Mechanism and Machine Science (CD), Taipei, Taiwan. 2010.

Kiper, Gökhan. "ME 573- Deployable Structures." Lecture, İzmir Institute of Technology, Izmir, Turkey, Winter Semester, 2018.

Langbecker, Travis. "*Kinematic Analysis of Deployable Scissor Structure S*." International Journal of Space Structures 14, no. 1 (1999): 1-15. doi:10.1260/0266351991494650.

Langbecker, Travis, and Faris Albermani. "*Foldable positive and negative curvature structures: geometric design and structural response*." Journal of the International Association for Shell and Spatial Structures 41, no. 3 (2000): 147-161.

Langbecker, Travis, and Faris Albermani. "*Kinematic and non-linear analysis of foldable barrel vaults*." Engineering Structures 23, no. 2 (2001): 158-171.

Liao, Qizheng, and Li Duan Ling. "*Mechanisms For Scaling Planar Graphs*." Chinese Journal of Mechanical Engineering 41, no. 08 (2005): 140. doi:10.3901/jme.2005.08.140.

Maden, Feray, Koray Korkmaz, and Yenal Akgün. "*A Review of Planar Scissor Structural Mechanisms: Geometric Principles and Design Methods*." Architectural Science Review 54, no. 3 (2011): 246-57. doi:10.1080/00038628.2011.590054.

"NuSTAR Now Accepting Cycle 4 Proposals" The Nuclear Spectroscopic Telescope Array science operations center. Last modified November 20, 2017. https://www.nustar.caltech.edu/news/90

Piñero, Emilio Pérez. "*Project for a Mobile Theatre*." Architectural Design 12 (1961a): 154-55.

Piñero, Emilio Pérez. "*A Reticular Movable Theatre*." The Architects' Journal 134 (1961b): 299.

Piñero, Emilio Pérez. Three Dimensional Reticular Structure. US Patent 3,185,164, issued May 25, 1965.

Robbin, Tony. *Engineering a New Architecture*. New Haven: Yale University Press, 1996.

"ROK" ROK, Rippmann Oesterle Knauss GmbH. Accessed June 27, 2018. http://rok-office.com/projects/0800-pininfarina/

"Rolling Bridge" Heatherwick Studio: Design & Architecture. Accessed June 27, 2018. http://www.heatherwick.com/project/rolling-bridge/

"Roman Furniture", Pinterest. Accessed July 02, 2018. https://tr.pinterest.com/pin/358176976600092002/

Söylemez, Eres. "*Using computer spreadsheets in teaching mechanisms*." In *EUCOMES 08*, 45-53. Proceedings, Dordrecht, Netherlands. Springer, 2008.

Van Mele, Tom, Niels De Temmerman, Lars De Laet, and Marijke Mollaert. "*Scissor-hinged Retractable Membrane Structures*." International Journal of Structural Engineering 1, no. 3/4 (2010): 374. doi:10.1504/ijstructe.2010.033489.

Yar, Müjde. *Design of Novel Transformable Planar Structural Linkages with Angulated Scissor Units*. Master's thesis, İzmir Institute of Technology, 2016.

Yar, Müjde, Koray Korkmaz, Gökhan Kiper, Feray Maden, Yenal Akgün, and Engin Aktaş. "*A novel planar scissor structure transforming between concave and convex configurations*." International Journal of Computational Methods and Experimental Measurements, Vol. 5/4 (2017): 442. doi:10.2495/CMEM-V5-N4-442-450

You, Z., and S. Pellegrino. "*Foldable Bar Structures*." International Journal of Solids and Structures 34, no. 15 (1997): 1825-847. doi:10.1016/s0020-7683(96)00125-4.

Zhang, Ran, Shiwei Wang, Xuejin Chen, Chao Ding, Luo Jiang, Jie Zhou, and Ligang Liu. "*Designing Planar Deployable Objects via Scissor Structures*." IEEE Transactions on Visualization and Computer Graphics 22, no. 2 (2016): 1051-062. doi:10.1109/tvcg.2015.2430322.